Spring 5-1-2023

Using Cesium-137 to Determine Sedimentation Patterns in Two Proglacial Lakes - Lago Argentino, Argentina, and Lake Josephine, Montana, USA

Louis Miller
lmiller8@macalester.edu

USING CESIUM-137 TO DETERMINE SEDIMENTATION PATTERNS IN TWO PROGLACIAL LAKES - LAGO ARGENTINO, ARGENTINA AND LAKE JOSEPHINE, MONTANA, USA

A THESIS PRESENTED TO THE DEPARTMENT OF

GEOLOGY

MACALESTER COLLEGE

14 April 2023

IN PARTIAL FULFILLMENT OF THE REQUIREMENTS FOR THE SENIOR HONORS PROGRAM

BY: LOUIS MILLER

FACULTY ADVISOR: DR. KELLY MACGREGOR

Contents

Figures

Tables

1 Abstract

Glaciers are a key driver of bedrock erosion and sediment transport in alpine settings, and subsequent sediment deposition in proglacial lakes records glacial retreat, subglacial erosion rates, and other evidence of environmental change, like wildfires. Sedimentation in these proglacial lakes can reflect a variety of processes and characteristics such as glacier and lake size, proximity to the glacier, depositional patterns, other sources of sediment in the basin, and summer melt rates. Accurate dating of lake sediments in glacial systems can be challenging, particularly on sub-millennial timescales due to limited terrestrial organic matter in these environments. Atmospheric fallout of cesium-137 from aboveground nuclear weapon detonation has been used as a tracer for modern sediment age and deposition rates in northern hemisphere terrestrial landscapes; fewer studies have been done in the southern hemisphere, especially farther south than 50° S, and results are likely complicated by lower atmospheric concentrations recorded there. Peak cesium-137 activity in the cores is an approximate equivalent for peak atmospheric radionuclide fallout from 1962-1965 (Garcia Agudo et al., 1998). Here I analyze a downvalley transect of cores from two alpine lakes, the 100 km long ice-contact Lago Argentino in Argentina and from 2 km long Lake Josephine in Glacier National Park, Montana, the third in a series of paternoster lakes, to assess downvalley variability in sedimentation rates in two endmember glacial lake types.

Gamma-ray spectroscopy was used to measure cesium-137 decays at 2 mm to 1 cm intervals, which was converted to specific activity based on dried sample weight. In Lago Argentino, analyzed cores showed average post-1963 sedimentation rates from 23 mm/yr 20 km from the ice front, to 2.3 mm/yr 80 km downvalley in the main basin (after Van Wyk de Vries et al., 2022). Preliminary results suggest high and episodic sedimentation in ice proximal settings may complicate cesium-137 interpretation. At Lake Josephine, sedimentation rates varied from 0.4-0.8 mm/yr on the upvalley side from cesium-137 and lead-210 dating (Diener, 2015)

to 0.4-0.5 mm/yr on the downvalley end using radiocarbon ages (Wydeven, 2009). While it is unlikely sediment production and delivery rates are consistent during this period of climatic variability, these rates are similar to average sedimentation rates found for this lake during the Younger Dryas and early Holocene based on bracketing volcanic ash ages. As expected, cesium-137 concentrations were higher in the North American glacial lake, but southern hemisphere levels were high enough to detect using standard techniques, and coupled with other tools such as varve counting (Van Wyk de Vries et al., 2022) provide a useful dating tool in glacial lakes.

2 Introduction

2.1 Proglacial lakes

Glacial lakes are most commonly formed by either glacial erosion that creates bedrock overdeepenings, which are subsequently filled with water during ice retreat, or by deposition of terminal or recessional moraines blocking water flow downvalley. Advancing glaciers effectively bulldoze any topography in their path, flattening it and isostatically depressing it. As they retreat, they expose areas of low topography where lakes can form as a result of meltwater from the glacier. A proglacial lake is specifically a lake that lies downstream of a glacier, as opposed to lakes like the Great Lakes that were formed by glaciers that no longer exist (Larson and Schaetzl, 2001).

Subsequent transport and deposition of sediment in proglacial lakes provide a semi-continuous record of geomorphic processes in and around the lake, including glacial erosion and sediment transport to the lake. Because they have a semi-continuous deposition, they offer a semi-continuous history. We can learn about glacial retreat, subglacial erosion, even wildfire history of the area. Sedimentation also depends on factors other than rates of erosion. Sizes of both the lake and the glacier(s) feeding it, glacier proximity, additional sediment sources, and variable melt rates are some of the other major factors affecting sedimentation rates in proglacial lakes. Even with additional sediment sources, subglacial erosion still dominates sediment fluxes in proglacial lakes (e.g., Schachtman et al., 2015).

2.2 Glacial Erosion

Studies of glacial erosion help to understand glacial retreat and landscape evolution, since it is one of the most powerful eroders of rock. Glaciers erode bedrock by plucking and abrasion, either the ice itself doing the eroding or chunks of rock in the ice scraping along the bottom. Plucking is the process of ice removing bedrock as the glacier flows over it (Swift et al., 2015). This creates coarse ma-

terial initially, which can then be abraded into finer sediments. Abrasion occurs when the coarser fragments are entrained and pushed against bedrock by the ice, creating much finer sediments. This results in fine sediments being transported down the glacier and out into proglacial lakes. This process is one of the most effective forms of erosion, eroding about one to ten millimeters per year (e.g., Riihimaki et al., 2005; Swift et al., 2015). Over longer timescales, glacial erosion is typically estimated using numerical models, using variables such as topography, mass balance, cross-sectional area, and average ice velocities (e.g., MacGregor et al., 2000). Short timescale glacial erosion can be measured through sediment evacuation rates, where turbidity in the glacial stream is measured to estimate the amount of sediment being eroded by the glacier (Riihimaki et al., 2005).

2.3 Dating Techniques

Radiometric dating is a common form of dating lake sediment cores. Lead-210 is a naturally occurring radioisotope in the long decay chain of uranium-238. Lead-210 directly comes from gaseous radon-222, which rises through the crust and into the atmosphere before decaying into lead-210 and being deposited on the surface (Van Metre, 2004). Due to the half-life of lead-210 being 22 years, it is only able to be used for dating sediments within the past 75-100 years, after which there would not be enough of it left to reliably detect. At present, lead-210 allows us to look back farther in time than cesium-137, but only for another approximately 40 years. After that, the cesium-137 record would go back farther, and with a half-life of 30 years, cesium-137 from 1963 will be around and be detectable longer than lead-210 from the same time.

Varves are annual layers commonly seen in glacial lake sediments. They are characterized by alternating light and dark laminae, where one layer is primarily denser material deposited during times of higher energy in the system (summer), and the other layer when there is less energy in the system (winter). Typically, the winter layer is darker because it contains dead organic material compared

to the lighter, sediment-heavy summer laminae. This is not the case in Lago Argentino, because there is very little organic matter present. Instead, the darker layers represent the summer, because denser minerals are able to settle out of suspension then. Denser intervals correspond to more mafic minerals, and in the case of Lago Argentino, this is pyroxene-rich beds in the summer, and potassium feldspar-rich beds in the winter (Van Wyk de Vries et al., 2022). Varves are seen in cores throughout Lago Argentino, though they are not present in all of them (Van Wyk de Vries et al., 2021). The cores that do not have reliably annual sediment couplets in Lago Argentino (e.g., Core 33A) attribute their variation to multiple large-scale events that take place within a year, creating multiple layers during the time span in which only one would be created. Varves are not seen in Lake Josephine, bedding couplets make up multi-year scales.

I want to look at sedimentation in very recent time scales. For Lago Argentino, using carbon-14 dating for a longer history would have been futile, since there was little to no charcoal or other organic material present in any of the cores, a necessity for carbon-14 dating. Lead-210 is the other major isotope used for dating lake sediment cores. However, lead-210 dating requires specific sampling methods and preservation, whereas cesium-137 can be done on any samples.

2.4 Cesium-137

Cesium-137 is a radioactive isotope with no natural origin, only forming as a fission product of uranium-235. Cesium-137 is one of the more common fission products of uranium-235, with a yield of 6.1% (Plompen et al., 2006). It can either be formed directly, or as a product of decay of tellurium-137, iodine-137, or xenon-137. Cesium-137 has a half-life of 30.17 years, and once it is created, about 95 percent of it decays to barium-137m, and the other five percent decays to the more stable barium-137 (Figure 1). Barium-137m is then converted to barium-137, which emits gamma radiation at 0.662 MeV, the peak used for spectroscopy when finding cesium-137 in samples (Figure 2).

Above-ground nuclear detonations inject radioactive isotopes, like cesium-137, into the atmosphere. Wind currents then disperse it globally, though the Hadley and Ferrel cells prevent it from being an even distribution. A major outcome of these patterns is that it is very difficult for particles to transfer between the Northern and Southern Hemisphere. This circulation pattern also explains the higher concentration of cesium-137 in the mid-latitudes between 40° N and 50° N, as seen in Figure 3 (Agudo et al., 1998). Cesium-137 particles then adhere to particles in the atmosphere, which then fallout via precipitation, depositing them on the surface (Figure 4). Because the general timeline of nuclear detonations is known, the expected fallout history of radioactive isotopes is easily approximated. The peak of fallout of cesium-137 is from 1962-1965, though for this paper, 1963 is used for calculations. Above-ground nuclear detonations were banned in 1963, leading to the peak being in this time frame. The Northern Hemisphere sees an additional peak in the mid-1980s from the Chernobyl Disaster (Figure 5). Since it only comes from a human source, it is a reliable tracer in sediments for very recent timescales (over the past 60 years). Cesium-137 is much more concentrated in the Northern Hemisphere, because that is where a majority of nuclear testing happened, like Nevada Test Site, USA, Novaya Zemlya, USSR (present-day Russia), and Semipalatinsk, USSR (present-day Kazakhstan). In total, there have been 528 recorded atmospheric nuclear detonations between 1945 and 2017 (Kimball, 2022). When it lands, cesium adsorbs well to certain clay minerals like vermiculite and illite, but not well to others like montmorillonite (Hashimoto et al., 2013). This is because these clay minerals have negative charges on the outside of their structure, and cesium has a positive charge. This brings the two together, making cesium more abundant in clay-rich sediments. Cesium-137 can only be used over very recent timescales. Clay-rich sediments are needed to hold on to it. Another limitation is that, unlike carbon-14 dating, where only one sample is needed to date the core, cesium-137 dating requires each section of the core to undergo gamma spectroscopy for a date to be determined.

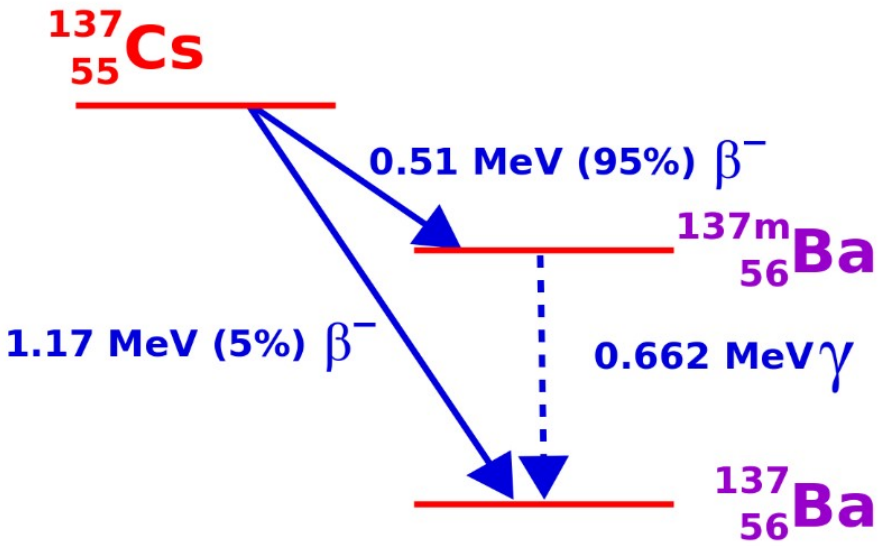

Figure 1: Decay scheme of cesium-137 to 137-barium, showing the energy of 0.662 MeV of gamma radiation.

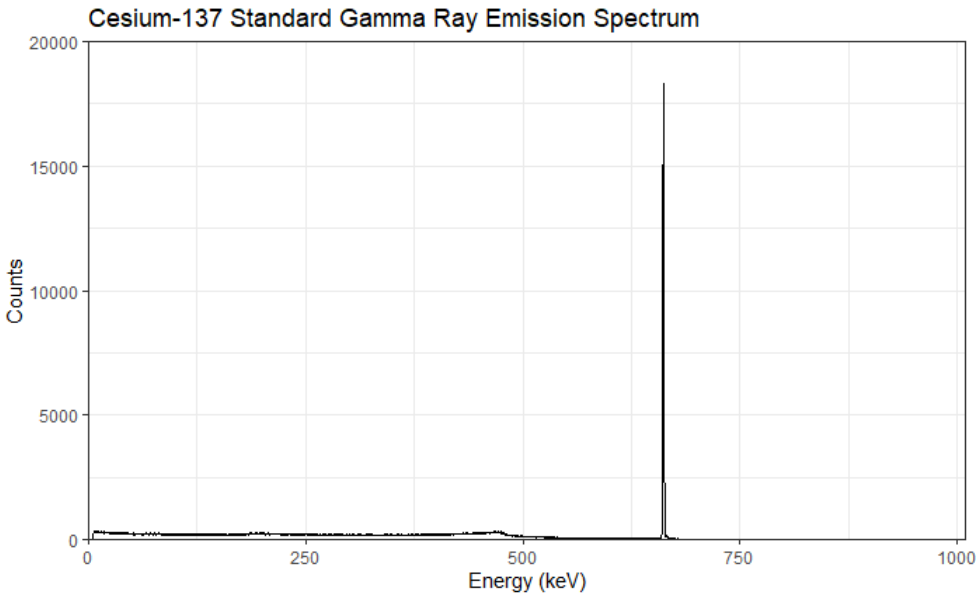

Figure 2: Gamma spectroscopy curve of a 10μg sample of cesium-137

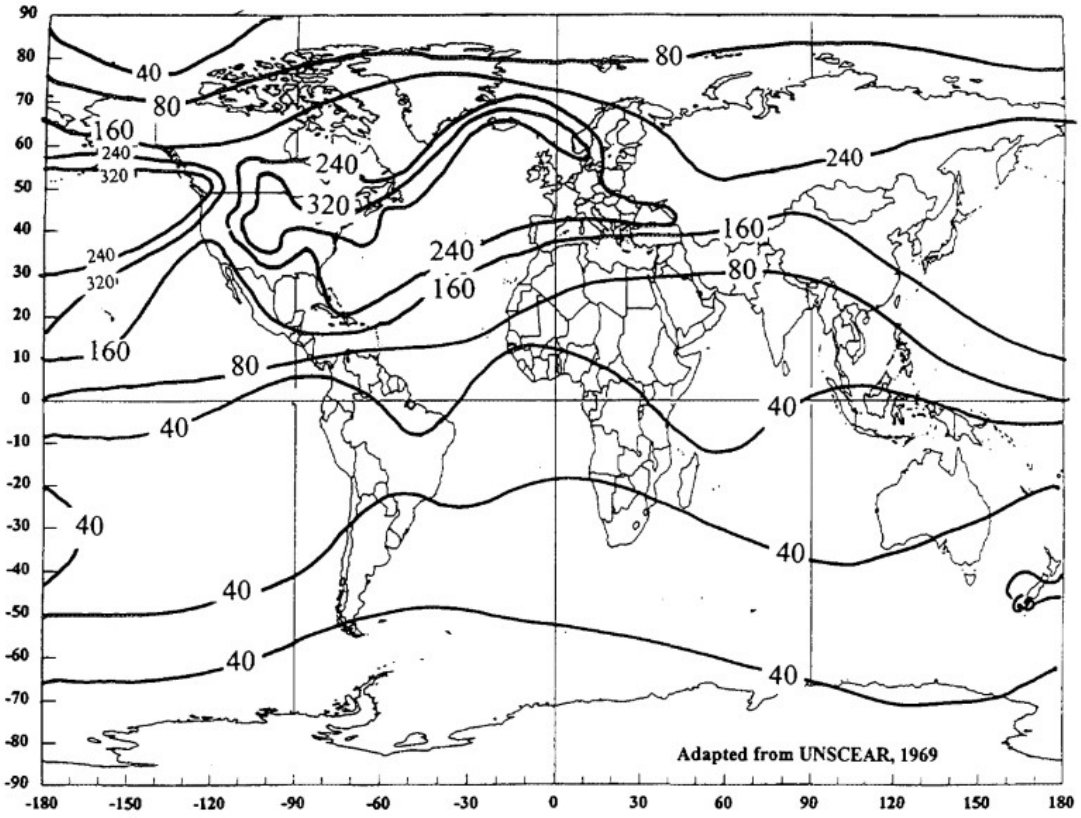

Figure 3: Estimate of global cesium-137 distribution in mBq/cm^2 as of 1996 (Agudo et al., 1998)

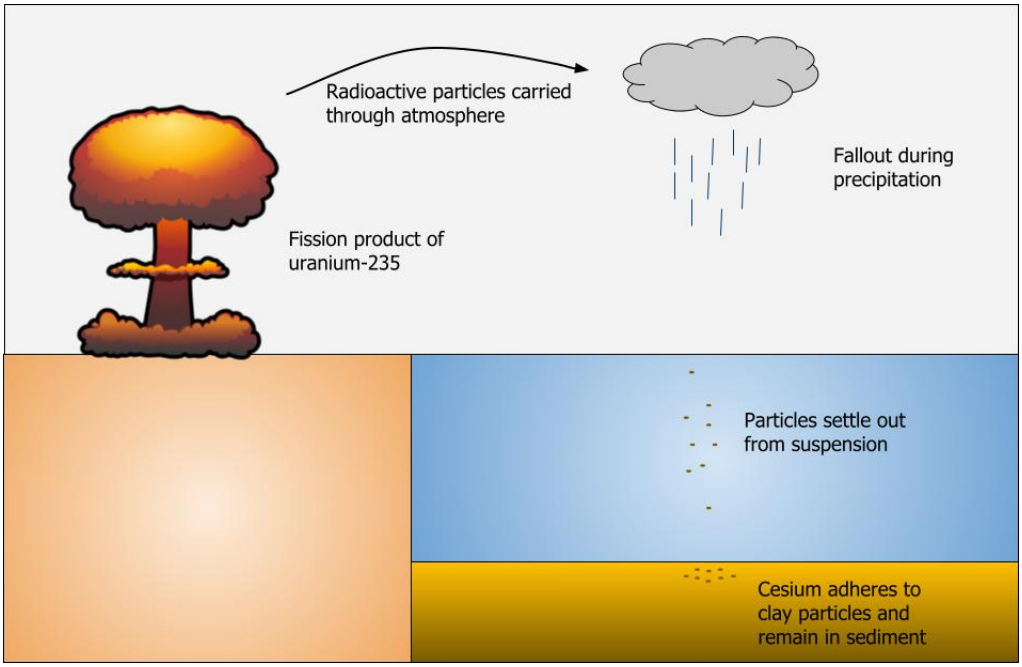

Figure 4: Graphic showing how cesium-137 gets dispersed and deposited

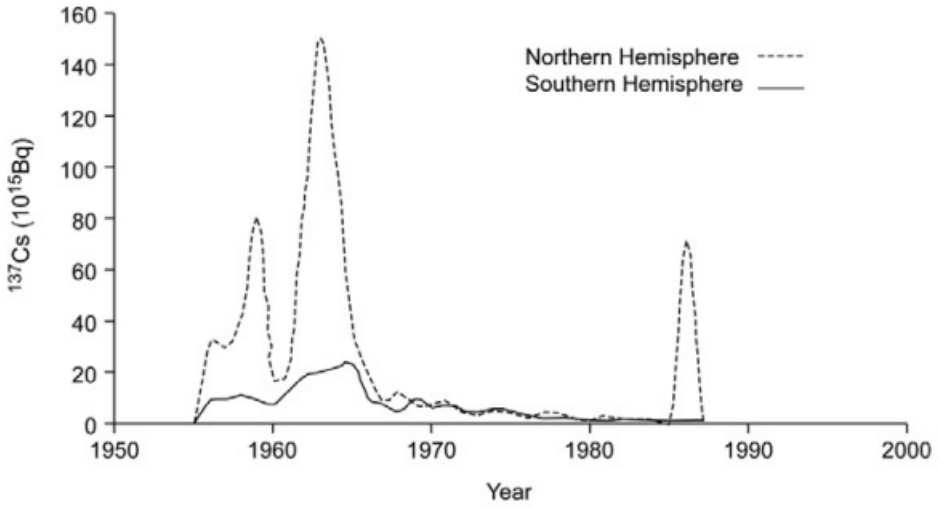

Figure 5: Estimation of overall cesium-137 deposition in both Northern and Southern Hemispheres (From Cambray et al., 1989).

2.5 Research projects

The Lago Argentino samples were part of a larger project investigating sedimentary properties and processes of proglacial lakes (Van Wyk de Vries et al., 2022). This itself is also part of a larger project determining the overall dynamics of the Southern Patagonian region, comparing glacial erosion to the high rates of uplift. The Lake Josephine cores are from Dr. Kelly MacGregor's ongoing research of the Many Glacier area's glacial history. Her research has looked at six different lakes in Grinnell and Swiftcurrent valleys, as well as studying Grinnell Glacier directly, in order to fully understand the processes of glacial movement and erosion in this alpine landscape. This has included inorganic carbon, wildfire charcoal, and pollen as proxies for landscape change. Overall, I am looking at lake dynamics through the lens of sedimentation rates over the past 60 years. This research confirms an input to output decrease in sedimentation rates in proglacial lakes, and finds that these two lakes have similar patterns despite differences of scale and climate.

3 Field Setting

3.1 Lago Argentino

Lago Argentino is the largest ice-contact lake in the world, located in southern Argentina in the Southern Patagonian icefield (Figure 6). The lake is fed by several glaciers in the icefield. This lake is over 500 meters deep at its deepest point, covering an area of 1,415 km^2. At 50° S, it is also one of the southernmost locations where cesium-137 dating has ever been done. The two major arms of the lake go north and south off the west end of the lake. Lago Argentino sits to the east of the Andes Mountains, where a fold-and-thrust belt caused the uplift of late Paleozoic to early Mesozoic sedimentary rocks (Coutand et al., 1999). Mostly, the basement rocks are Paleozoic and Jurassic siliciclastic rocks reaching 2000 meters thick: greywackes, quarzitic sandstones, and shales. In addition, volcanic

activity has created plenty of igneous deposits in and around the Lago Argentino area, including 1,000 meter thick deposits of the El Quemado complex, a felsic aphanitic volcaniclastic deposit (Iglesia Llano et al., 2003). There are three active volcanoes within 100 km of the lake as well (Coutand et al., 1999). The Rio Mayer formation, which consists of Cretaceous shales, is also part of the local geology (Figure 7) (Moyano-Paz et al., 2018).The glacial valleys that feed Lago Argentino have straight sides and have similar widths to each other and to those of nearby Lago Viedma and Lago San Martin, implying that they are defined not by glacial erosion, but by fault zones (Coutand et al., 1999). The glacial valleys that trend north-south are also structurally controlled, agreeing with the locations of thrust faults in Figure 7.

The Lago Argentino region had its Last Glacial Maximum 13,000 years before present (BP), and ice stretched to the eastern edges of the basin (Strelin et al., 2014). After that, the glacial field underwent a complicated pattern of retreat and advancement. The glaciers retreated deep into their valleys by 12,660 $\pm$ 70 years BP according to carbon-14 dating and beryllium-10 dating (Strelin et al., 2014). Seven other advances are theorized to have occurred since then from tree ring dating analysis of sedimentary sequences, the most recent of which being less than 300 years BP, none of which reaching the scale of covering the entire lake basin (Strelin et al., 2014). There are six glaciers that feed into Lago Argentino: Ameghino, Onelli, Mayo, Perito Mereno, Spegazzini, and Upsala. Of these, only three are ice-contact: Perito Moreno, Spegazzini, and Upsala.

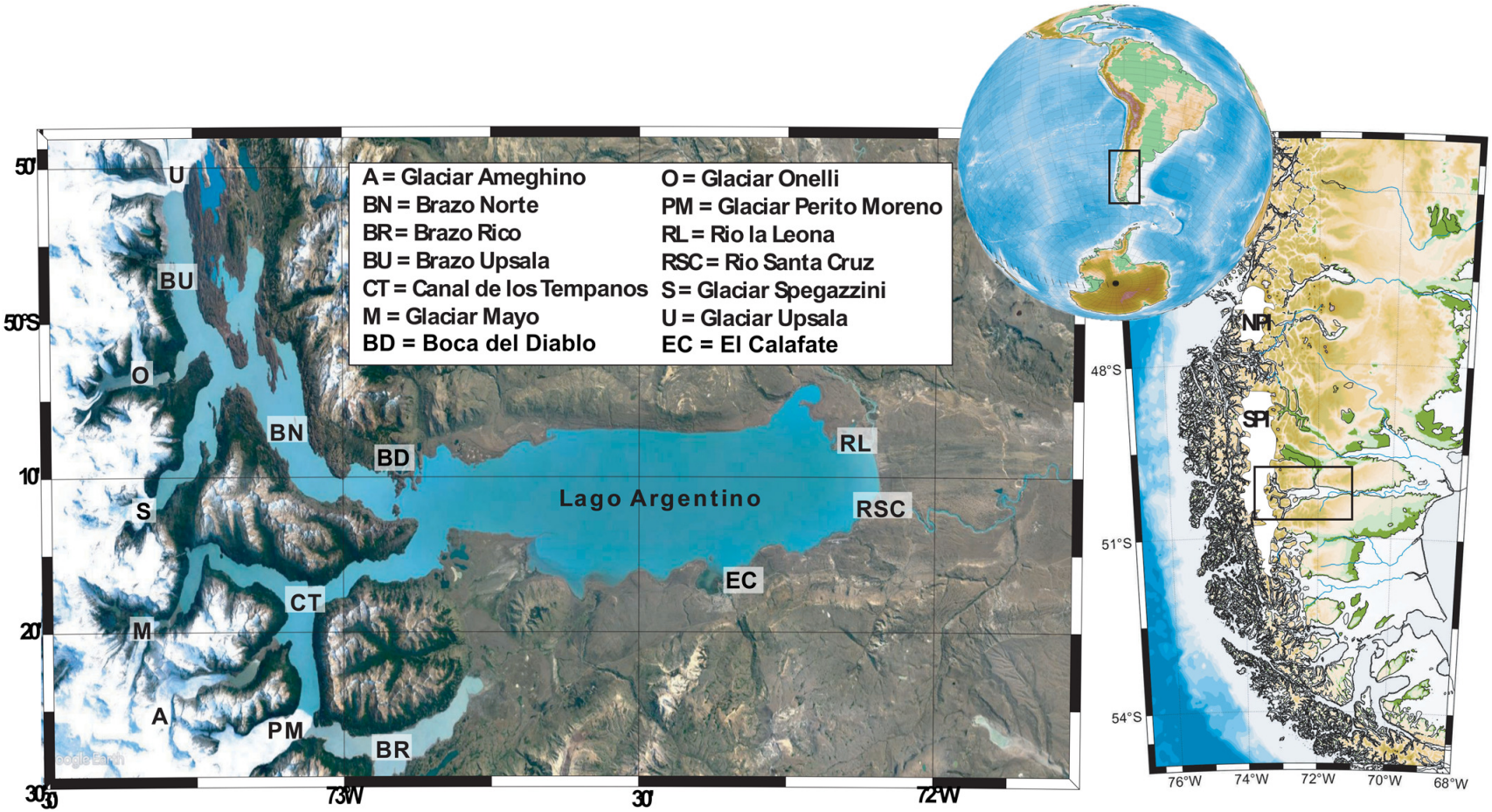

Figure 6: Map of Lago Argentino, showing location of key features of the lake (Van Wyk de Vries, 2022)

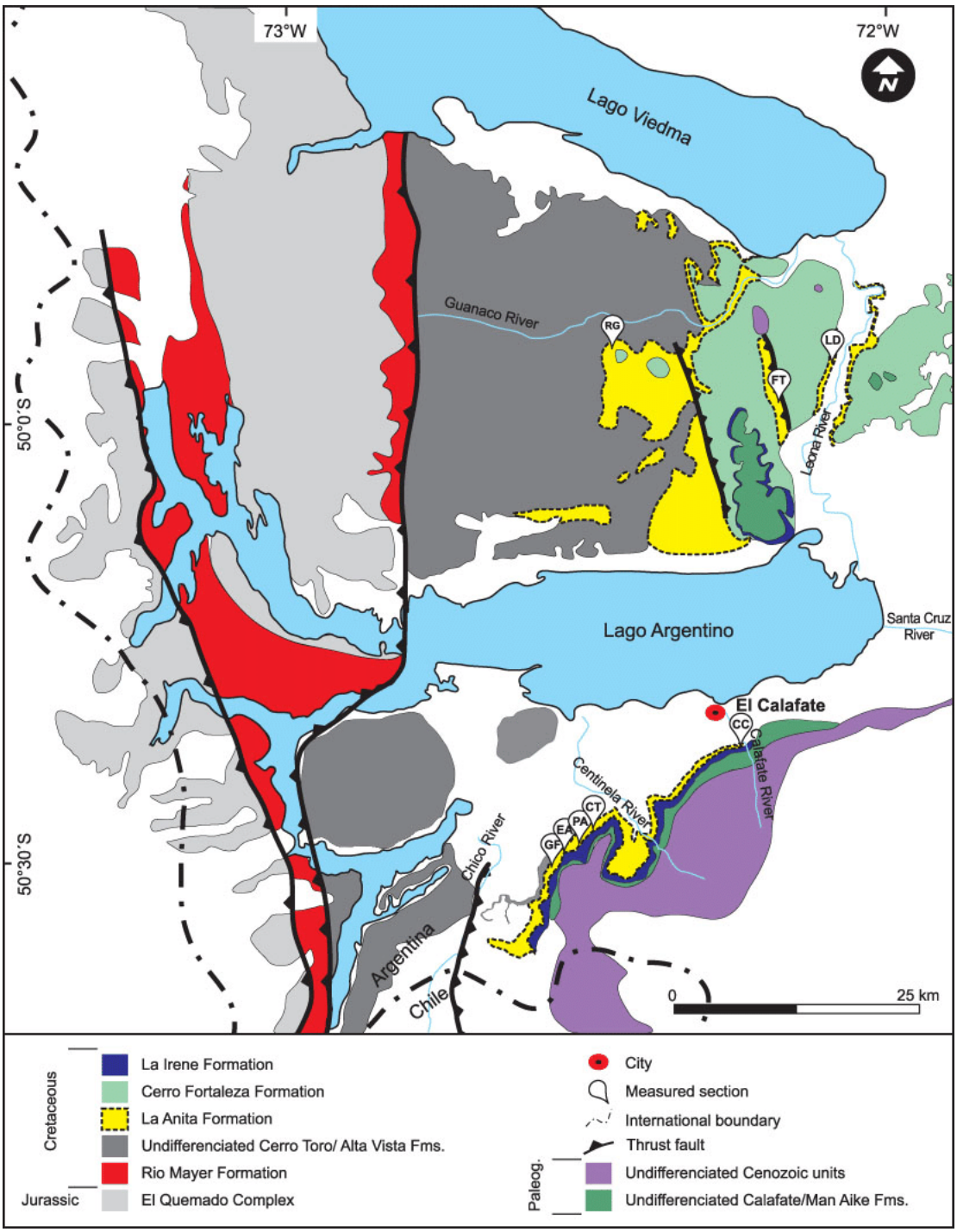

Figure 7: Geologic map of Lago Argentino, showing bedrock geology, as well as major structural features (Moyano-Paz et al., 2018)

3.2 Lake Josephine

Lake Josephine is in the eastern part of Glacier National Park in Montana on the ancestral home of the Blackfeet Nation. It is the third in a series of paternoster lakes in a glacial valley with Grinnell Glacier sitting at the top (Figure 8). The lake is 27 meters deep at its deepest point, and covers an area of 0.54 km^2. Lake Josephine has not been an ice-contact lake since approximately 18,000 years before present (Schachtman et al., 2015). Glacier National Park is in northwestern Montana, lies in the foothills of the Rocky Mountains, and is 4,100 km^2 in area. The Grinnell Valley is in the northeastern part of the park, and is approximately 36 km^2 in area.

The bedrock geology of the Grinnell Valley consists mostly of Precambrian sedimentary rocks. Sedimentation began 1.6 billion years ago, when the Belt Sea covered present day eastern Washington, northern Idaho, and eastern Montana (NPS, 2020). In total, 5,500 meters of sediment were deposited, consisting of arenite, argillite, and limestone. These rocks range in color from yellow to green to red (leading to the namesake of Redrock Lake in the neighboring Swiftcurrent Valley). The only fossils present in the Grinnell Valley are the stromatolites found in the Siyeh and Altyn Formations, which are the more calcareous of the formations. Uplift then started 70 million years ago, when the Lewis Thrust Fault pushed bedrock 80 km east. This was caused by crustal collisions that formed what is now the West Coast.

The many glaciations during the Pleistocene likely played a role in the creation of the glacial erosional and depositional features in the Rocky Mountains (NPS, 2020). The Grinnell Valley was created by the advance of Grinnell Glacier, carving out the valley that now hosts four glacial lakes: Upper Grinnell Lake, Grinnell Lake, Lake Josephine, and Swiftcurrent Lake (Figure 8). These lakes were created during the retreat of the glacier, where the glacier preferentially eroded softer rock, leaving a lake to sit in the basin, while harder rocks were less eroded and created a natural dam (Glacier Natural History Association, 2008).

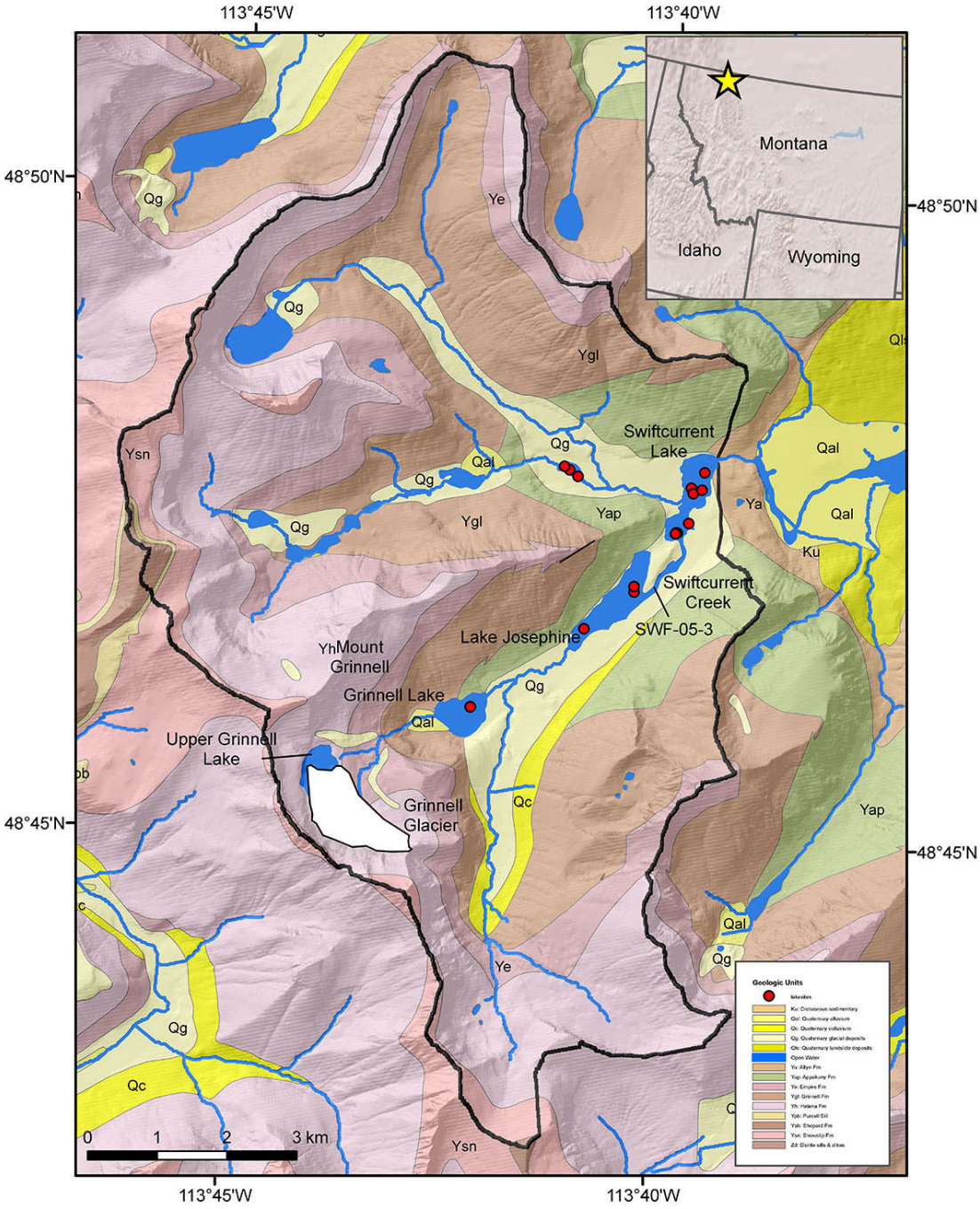

Figure 8: Geologic map of the Many Glacier area, with Grinnell Valley and Lake Josephine in the center. The red dots represent a core location, though only cores from Lake Josephine were used in this study. Image from the Keck Consortium

Grinnell Glacier sits at the top of the Grinnell Valley, where it contacts Upper Grinnell Lake. It is a small glacier, only 0.62 km^2 as of 2005, and has certainly shrank more in the 18 years since. Other than Grinnell Glacier, Salamander, Gem, and Swiftcurrent Glaciers are all named glaciers in the Many Glacier area. However, they are all under the area limit of 0.1 km^2 that the USGS uses to delineate a glacier from a large snowpack. Salamander and Gem Glacier both are shelf glaciers that once connected to a larger Grinnell Glacier. The glaciers were separated some time before 1929, when repeat photography had begun on the glacier.

4 Methods

4.1 Field Methods

4.1.1 Lago Argentino

Due to the vast size difference between the two lakes, core acquisition was different for each. The Lago Argentino coring expedition took place during the (Southern Hemisphere) winter, when winds were lower (Van Wyk de Vries et al., 2022). Lower winds are important for both boat stability, and fewer icebergs, which is necessary for the glacier proximal cores. A vehicle ferry was used for transportation around the lake, allowing for an A-frame to be built, necessary for Kullenberg coring. The coring devices used were a Kullenberg piston-coring system and a gravity surface coring device. A Kullenberg corer relies on gravity to push a polycarbonate-lined steel tube into the sediment, driven by a 1,000 pound lead weight on the core head (CSD Facility, 2023). Kullenberg systems are good for getting up to 12 m of sediment in deep lakes, as they are only limited by the amount of cable attached to them. However, because they are so heavy, they require a robust apparatus to pull them back up. Only two cores in this study used Kullenberg systems (LARG19-33A and LARG19-20B). The other coring device used in Lago Argentino were gravity surface corers like HTH corers and MUCK

corers. While Kullenberg, HTH, and MUCK devices are all gravity corers, HTH and MUCK preserve the sediment-water interface, where Kullenberg devices tend to disturb it.

Core Descriptions

All of the cores taken from Lago Argentino were done by a team associated with Van Wyk de Vries et al. (2022). Core 33A was the most glacier-proximal of the four cores in this study. It was taken at a water depth of 530 meters on September 4, 2019. It is 4.32 meters long, but only the top 140 centimeters are used in this study. Because of the 17 cm of space left for the sediment-water interface, there is 123 cm of sediment present that was studied. Core 27A was taken from the mixing point of the arms in the west of the main basin. The water depth at this location was 385 meters when the core was taken on August 30, 2019. The core is 67 cm long, though only 57 cm of it is actual sediment, and only the upper 37 cm of it were used for spectroscopy. Core 11A was the most glacial-distal core, and it is from the western side of the main basin. It was taken at a water depth of 99 meters on August 18, 2019, and is 30.7 cm long. 20A/B is from a side bay that not along the main transect. This core is a combination of GCO-LARG19-20A-1G and GCO-LARG19-20B-1K, taken from the same spot, but 20B goes deeper than 20A. A marker bed in each was used to correlate them, and 20B starts 5.7 cm deeper than 20A. Cores 20A and 20B were collected in 100 m water depth on August 23, 2019.

Van Wyk de Vries et al. (2022) did petrographic smear slides to more closely examine mineral content and grain size. They have a bimodal distribution of grain sizes, where one mode is sub-micron scale, and the other is from 1-10 μm. No minerals could be identified in the smaller of the modes without using higher resolution instrumentation than a petrographic microscope. The larger mode consisted of plagioclase, quartz, one to two pyroxenes, biotite, opaque oxides, and volcanic glass. Few diatoms were present, both centric and pennate, and they were more concentrated in the main basin than in the arms.

4.1.2 Lake Josephine

Both of the cores in Lake Josephine were collected from a Cataraft floating platform, with a metal casing running from the lake bed to the platform to guide the core collection and retrieval (Diener, 2015). Push corers like Livingstone and Bolivia corers were used to collect both of the samples present in this study. Livingstone and Bolivia corers both follow the same principle, metal drive rods are screwed on to the top of the core, and then they are pushed into the sediment by a team of 3-5 people (CSD Facility, 2023). Push corers are only useful in shallower waters, up to at most 50 m in depth, so the 16 meters maximum depth of Lake Josephine is no issue. They are also easier to transport than devices like Kullenberg systems, important since Glacier National Park does not allow wheels on their trails. Similar to gravity surface corers used in Lago Argentino, push coring devices maintain the sediment-water interface.

Core Descriptions

Cores from Lake Josephine were taken by undergraduate research groups through the Keck Consortium, one in 2010 and another in 2014. Core GNP-JOS14-1C-1P was located about 280 m downvalley from the input. Here, the water depth was 8.4 m when the core was taken on July 28, 2014. The core is nearly 15 meters in length, but only the top 20 centimeters were used. JOS14-1D was also taken at the same location, with the intended purpose of lead-210 dating. GNP-JOS10-2A-1P is from the downstream side of Lake Josephine, about 1.1 km from the inlet, and 150 m from the outlet. The water depth was 15.6 m on July 6, 2010, when the core was collected, and it had 6.12 m of sediment, though less than 10 cm were actually used for cesium-137 dating.

4.2 Lab Methods

4.2.1 Core Processing

In both lakes, cores were selected in a transect from upvalley to downvalley to examine changes in sedimentation rate at various distances from the main input source of sediment (glacier in Lago Argentino, river in Lake Josephine). For Lago Argentino, this meant one close to the glacier front (33A), at the western end of the main basin (27A), and one in the center of the main basin (11A). The last one, 20A/B, was not in the line of the transect, as it is in a side bay in a fjord without a glacier at the top, this site was chosen as a part of work done by Van Wyk de Vries et al. (2022) in verifying if laminae couplets in Lago Argentino were varves or not. The Many Glacier area in Glacier National Park has five different lakes with previous coring done: Lower Grinnell Lake, Lake Josephine, Redrock Lake, Fischercap Lake, and Swiftcurrent Lake. Of these, Lower Grinnell Lake does not have a transect of cores down it, Swiftcurrent takes in sediments from two different glacial valleys, and Fishercap and Redrock are both too small. This leaves Lake Josephine as the best lake to examine from the Many Glacier area, as it is the largest that only takes in sediments from one valley, and it has a vertical transect of cores.

Cores were brought back to the Continental Scientific Drilling Facility at the University of Minnesota-Twin Cities campus for analysis, sampling, and archiving. After the cores had been split and processed, they were sampled (Figure 9). Depending on the expected sedimentation rates of the cores, they were sampled from 0.2 cm to 1 cm increments for gamma spectroscopy. Expected sedimentation rates were determined in Lago Argentino via varve counting, and in Lake Josephine by previous carbon-14 work (Van Wyk de Vries et al., 2022; Schachtman et al., 2015).

Processing includes the use of a Geotek Multi-Sensor Core Logger (MSCL). Most notably, this takes the density of the core along its length in 0.5 cm increments. Density can be used as a proxy for clay content at each depth, as denser intervals have higher clay content, because clay is able to pack tighter and allow

Figure 9: Examples of core samples. Samples from Lago Argentino were put in mag boxes (left), and samples from Lake Josephine were put in polycarbonate containers (right).

for less porosity (Revil et al., 2002). The Geotek MSCL measured density by firing a beam of gamma rays from a sample of cesium-137 through the core (Geotek, 2023). This process is unrelated to the process of cesium-137 dating. The amount of rays that reach the sensor on the other side of the core can be used to calculate the density.

4.2.2 Cesium-137 Dating

Cesium-137 activity in lake core sediment samples was measured using a Canberra high-resolution, hyperpure germanium coaxial gamma detector (GC1518). The detector is surrounded by layers of copper, cadmium, and lead so that the detector is protected from background radiation. Sediment samples were collected from lake cores at the Continental Science Drilling facility at the University of Minnesota and were placed in u-channel segments or plastic mag boxes; neither container showed measurable cesium-137 activity when run as blanks. Samples were placed on the center of the detector for 12-48 hours, depending on approximate sample size. Using a cesium-137 standard with a calculated reduced activity based on standard age, I estimate a relative detector efficiency of 40% and a

resolution of 0.27 keV, similar to other gamma spectrometers. Resolution of the detector refers to the "bin size" for the spectrum. For example, the bin including the cesium-137 peak records anything with an energy between 661.7 and 661.97 keV. Using the relative efficiency of the detector, total values of cesium-137 could be determined. However there is not much to be gained from that, since I am most interested in relative levels within the same core. While overall detector efficiency can be calculated, measurements of cesium-137 in cores are primarily useful in documenting peak activity rather than absolute concentration. Additionally, sample geometry was different for each core and each lake, as sample boxes were different shapes for Lago Argentino and Lake Josephine. Also, if more than one sample was being run at a time, they could not perfectly share the detector stage, meaning efficiency was decreased when more than one sample was ran at a time. However, within a core, they consistently had the same amount of samples being run at a time. Count times provided an analytical precision of +/- 3% at the 95% confidence level. To determine dry sediment mass, samples were removed from their plastic containers, placed on aluminum trays, and dried in an oven at 110°C for 24 hours. Dry sample weights varied from core to core, dependent on sediment density and volume of sample, which includes the interval length and the size of sample (Table 1). Because the size of the sample in the dimensions other than that of the sample interval are unknown and inconsistent, the dry weights cannot be used to estimate the dry density of samples.

Core	Sample Interval (cm)	Range of Dry Weight (g)	Average Dry Weight (g)
33A	1	0.57 - 5.94	4.32
27A	0.5	0.52 - 2.34	1.37
11A	0.2	0.25 - 0.76	0.55
20A	0.5	0.59 - 3.40	1.74
20B	1	3.04 - 4.73	3.39
JOS14-1C	1	0.42 - 0.94	0.66
JOS10-2A	0.5	0.36 - 0.74	0.53

Table 1: Table summarizing sample intervals and dry weights of cores used.

Gamma ray spectroscopy is the method by which gamma decays are measured. Gamma ray spectrometers work by using high-purity germanium crystals that can convert gamma radiation into electrical signals. Germanium is used because it has a very low concentration of defects in its structure that affect electron movement (Fourches et al., 2018). Gamma rays interact with the electrons in the germaninum crystal, and voltage probes in the germanium crystal detect and measure these interactions. The system has to be cooled with liquid nitrogen (-196° C) so that the germanium crystal does not produce any erroneous signals. Because the detector cannot be cooled to absolute zero, there are still energy releases in the germanium crystal, which is seen as background noise whenever the detector runs. In order to prevent background radiation from the surroundings, the detector is encased in layers of copper and cadmium sheets, and lead bricks. These also serve to reflect radiation back into the germanium crystal. Samples were run for 12 hours for samples 10 cm or longer, 24 hours for 1 cm samples (most common), and 48 hours for samples less than 1 cm. Smaller sample intervals require longer runtimes because smaller samples on average have proportionally less cesium-137 activity, meaning it takes longer for a significant peak above background to develop.

To calculate sample activity in millibecquerels per gram (mBq/g), I determined background noise by averaging spectrum counts from 630.1-631.6 KeV and 690.1-691.4 KeV. This average was then subtracted from the cesium-137 peak at 661.7 KeV for the full-width at half maximum (FWHM) from 660.9-662.8 KeV based on the cesium-137 standard peak. The remaining values of above-background counts at the FWHM were summed to determine the true number of emissions (counts) for the sample. To convert counts (c) to sample activity (a) in becquerels/kg,

$$a = \frac{c}{t * m}. \tag{1}$$

Where a is specific activity, c is cesium-137 counts, m is dry mass in kg, and t is the length of the sample run in seconds.

To turn activity into sedimentation rates (SR), the peak activity in a core

corresponds to the year 1963, so the sedimentation rates for the past 50 or so years can be determined. Dividing the depth (l) of the sample with the peak activity by the number of years between 1963 and the date the sample was collected (t_1-1963) yields the rate of sedimentation (Equation 2).

$$SR = \frac{l}{t_1 - 1963} \tag{2}$$

5 Results

5.1 Lago Argentino

Four cores were studied in a transect from glacial proximal to glacial distal. All cores showed a significant peak that was able to be assigned as 1963. Core locations are shown in Figure 10.

GCO-LARG19-33A-1K (Figure 11) was the core from the site closest to the icefield, with the site being about 16 kilometers from the edge of Perito Moreno Glacier. Like all of the cores from Lago Argentino, it consists of alternating laminae of light and dark sediments. Unlike the other cores however, 33A does not appear to be varved, instead it has more than one laminae couplet per year. Evidence for ice rafting of larger sediments is available in this core, as a clast about 1 cm in diameter was found at 42 cm. GCO-LARG19-27A-1G (Figure 12) is located in the eastern part of the main basin, close to where the two main arms of the lake meet. Core 27A also has layering, except it was determined to be varves. GCO-LARG19-11A-1G (Figure 13) was the lightest in color, and the shortest of the cores. GCO-LARG19-20A-1G and GCO-LARG19-20B-1K (Figures 14 and 15) are not part of the transect, but they were varved cores in a side fjord without a glacier at the top.

Figure 10: Map of Lago Argentino showing the locations of the four cores. Core A is 33A, Core B is 20A/B, Core C is 27A, and Core D is 11A.

Figure 11: Core GCO-LARG19-33A-1G. The top of the core is the left side. Arching of the layers is due to forces within the tube, unrelated to the lake itself.

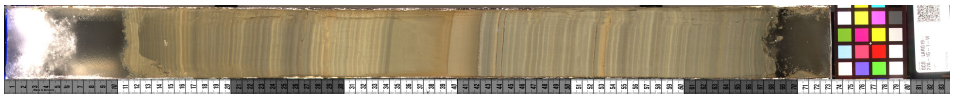

Figure 12: Core GCO-LARG19-27A-1G. The top of the core is the left side.

Figure 13: Core GCO-LARG19-11A-1G. The top of the core is the left side.

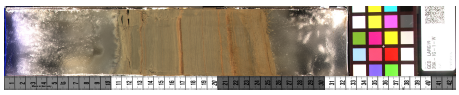

Figure 14: Core GCO-LARG19-20A-1G. The top of the core is the left side.

Figure 15: Core GCO-LARG19-20B-1G. The top of the core is the left side.

Core 33A had a significant activity peak at a depth of 125.6 cm (Figures 16 and 17), equivalent to a sediment depth of 108.6 cm (Figure 18). This core had the highest sedimentation rate at 19.4 mm/yr. Activity peaked at 0.31 millibecquerels per gram (mBq/g), and the lowest value seen was 0.0068 mBq/g. Values of 0 mBq/g were not seen in 33A, but the presence of the large peak in this sample window mostly rules out the potential for there to be significant activity deeper than this sample window. Figures 9 and 10 serve as a reference to the appearance of the spectrum of gamma radiation and the cesium-137 peak raw data, respectively. Figure 18 shows an increase in cesium-137 activity from 140 cm to 125 cm before a decrease until a plateau at approximately 98 cm. Specific activity stays around 0.02 mBq/g from a depth of 98 cm to the modern sediment at 17 cm (core 33A had 17 cm of Zorbitrol at the top).

Core 27A had a significant activity peak at a depth of 29.6 cm, equivalent to a sediment depth of 19 cm (Figure 19). Assuming constant sediment deposition and no erosion at this site between 1963 and 2021, the average accumulation rate here is 3.39 mm/yr. Cesium-137 activity peaked at 0.70 mBq/g, and was 0 mBq/g beneath a depth of 36.6 cm. Cesium-137 activity increases between a depth of 34.6 cm and 29.6 cm, after which it slowly decreases until 14.6 cm. Above 14.6 cm, cesium-137 activity increases up to 10.6 cm, which is the top of the sediment in the core.

Core 11A had a significant activity peak at a depth of 12.2 cm, equivalent to a sediment depth of 3 cm (Figure 20). 11A had the lowest sedimentation rate of Lago Argentino cores at 0.54 mm/yr. Specific activity peaked at 0.39 mBq/g, and no cesium-137 was detected below 17.2 cm. Activity increased between 14.2 cm and 12.2 cm, above which it decreased until the most modern sediment.

Cores 20A and 20B were combined, as the cesium-137 profile at the base of 20A (16.8 cm) did not reach 0 mBq/g, but it did within 20B. This profile had a significant activity peak at a depth of 15.1 cm, equivalent to a sediment depth of 4.5 cm (Figure 21). Similar to 11A, 20A/B had a very low sedimentation rate at

0.80 mm/yr. Activity peaked at 0.39 mBq/g, and was at 0 mBq/g below 20.6 cm.

Peak activity across the four cores from Lago Argentino ranged from 0.3 to 0.7 mBq/g. Figures 18, 19, 20, and 21 show the pattern of cesium-137 activity as a function of depth in each of the cores. All cores showed a rapid shift from low to high activity before a decrease to modern sediment values.

Core	Depth of Activity Peak (cm)	Sedimentation Rate (mm/yr)	Peak Activity (mBq/g)
33A	108.6	19.4	0.31
27A	19	3.39	0.70
11A	3	0.54	0.39
20A/B	4.5	0.80	0.39

Table 2: Table summarizing results of Lago Argentino cores.

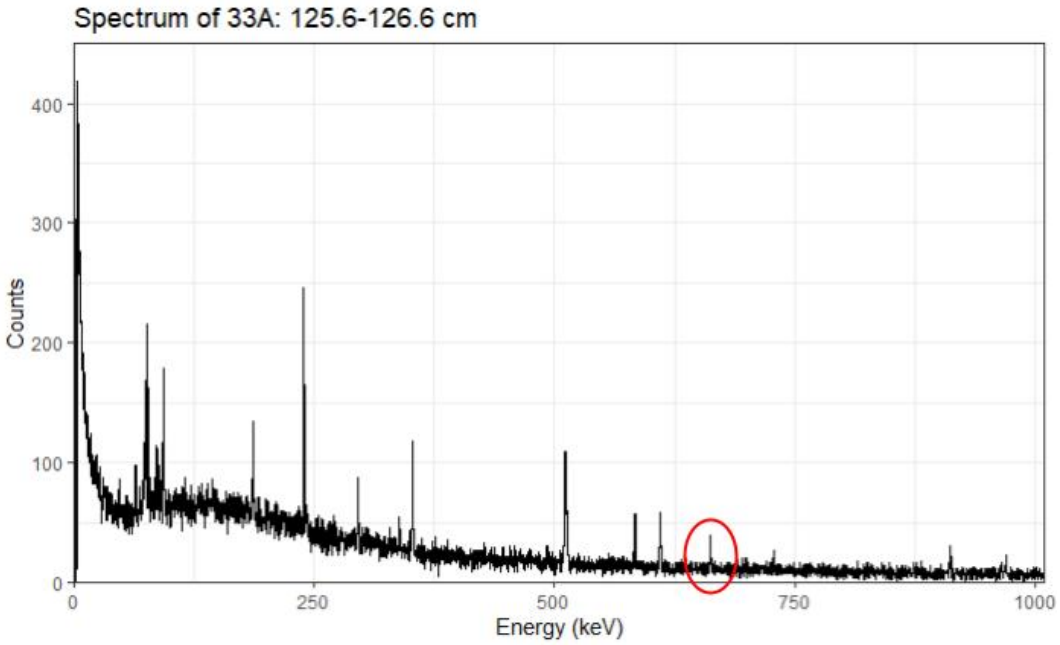

Figure 16: Gamma-ray spectrum of 125.6-126.6 of LARG19-33A. The cesium peak (red circle) is small compared to the whole spectrum.

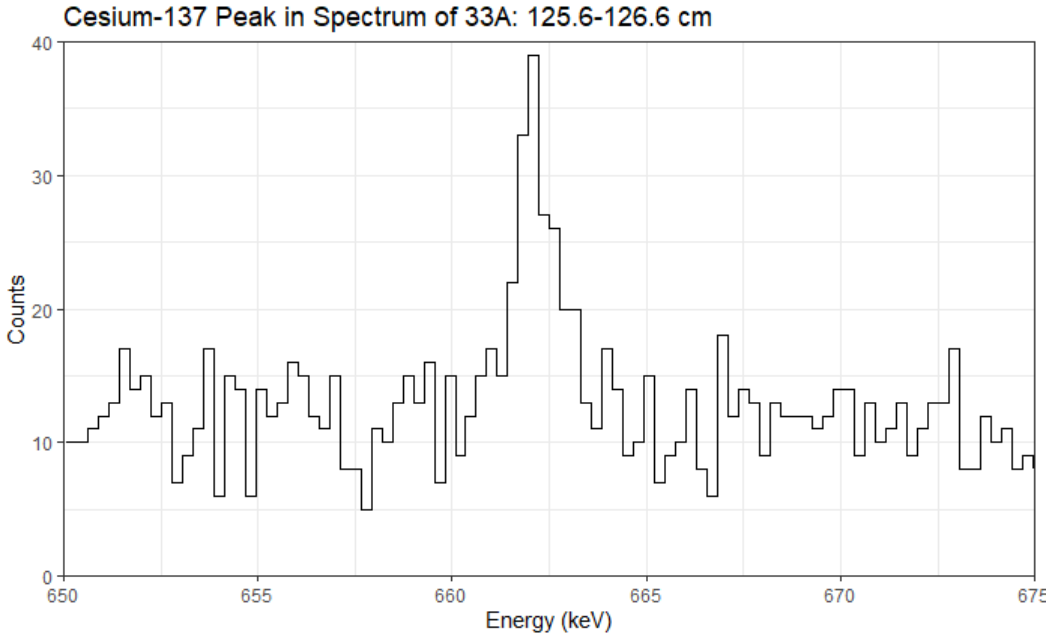

Figure 17: Cesium-137 Peak in 125.6-126.6 of LARG19-33A.

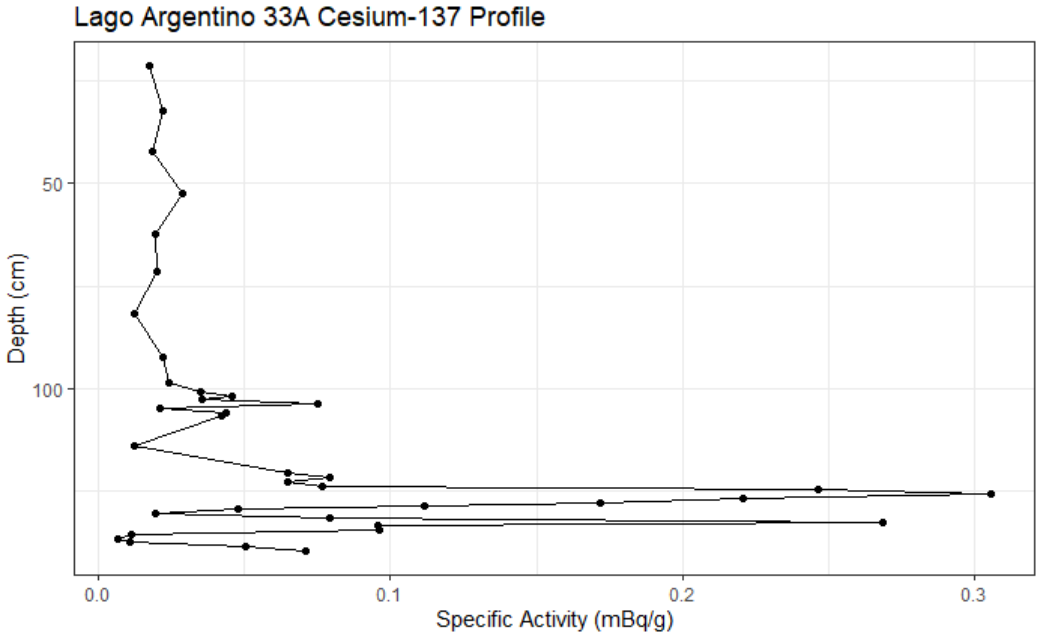

Figure 18: Cesium-137 distribution within core GCO-LARG19-33A-1G

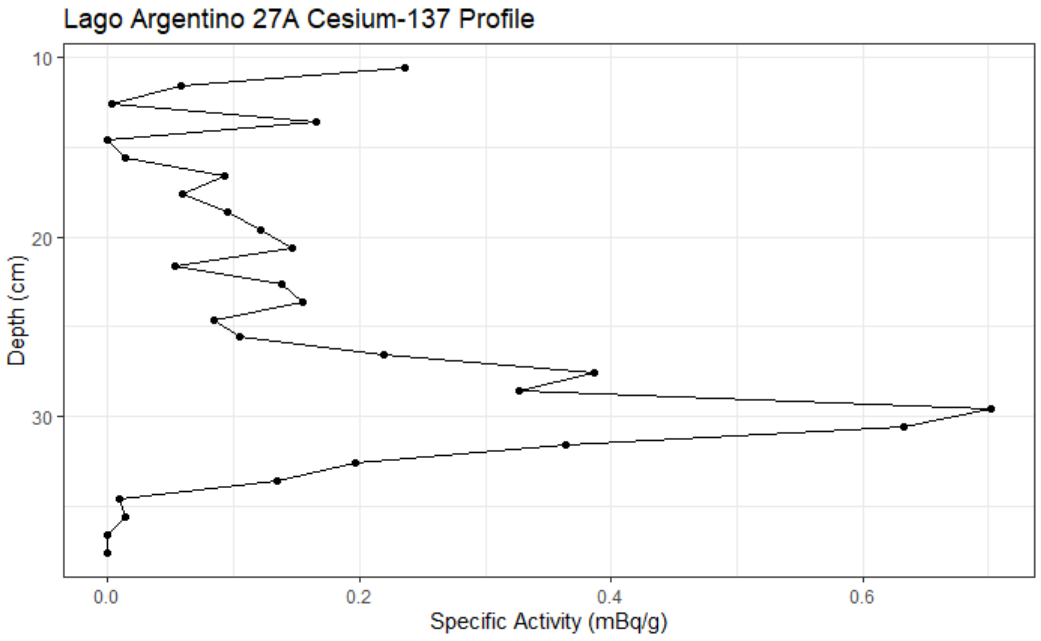

Figure 19: Cesium-137 distribution within core GCO-LARG19-27A-1G

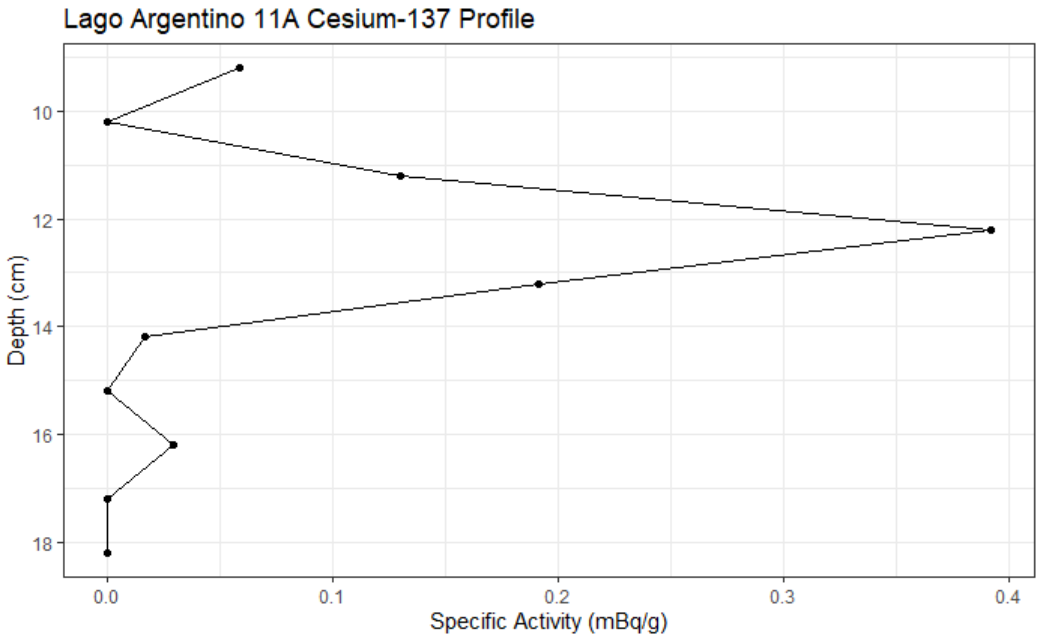

Figure 20: Cesium-137 distribution within core GCO-LARG19-11A-1G

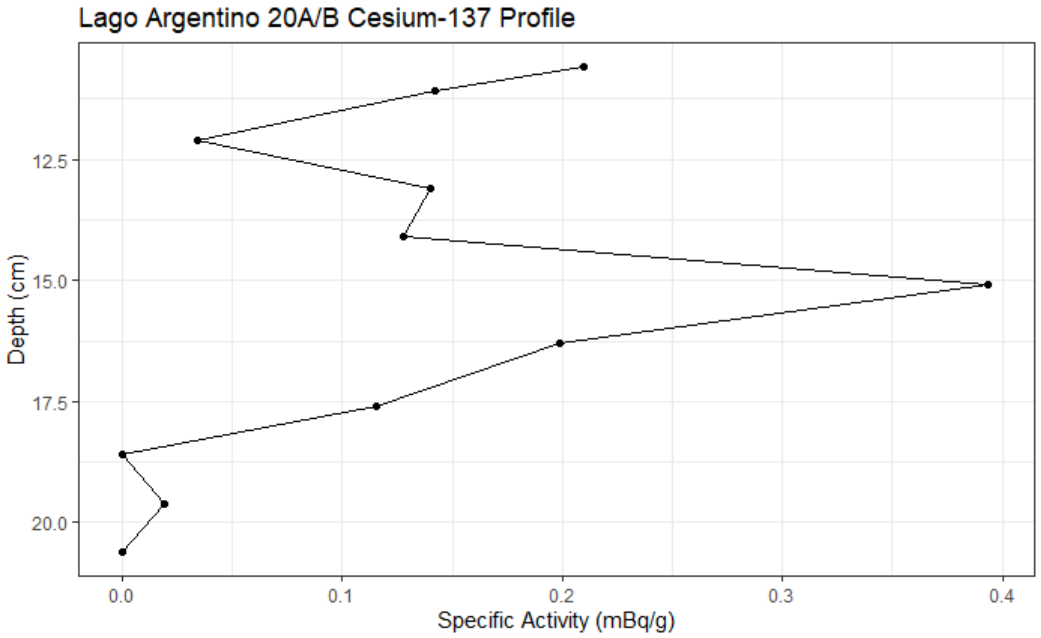

Figure 21: Cesium-137 distribution within core GCO-LARG19-20A-1G and GCO-LARG19-20B-1K

Density values from the Geotek MSCL allow us to look at whether or not cesium-137 presence is because of grain size, or if it is actual fluctuation in cesium-137 values. The absolute values of density are irrelevant, because density depends on more than just grain size, as water content and mineral composition are also factors. It is useful relatively within cores though, as in conjunction with initial core descriptions, it quantifies how sandy or clayey the sediment is. Each of the cores has a different range of densities, also each showing a different range of patterns. 33A varies from 1.72 g/cm^3 to 2.29 g/cm^3, with a range of 0.57 g/cm^3 (Figure 22). 27A varies from 1.38 g/cm^3 to 1.86 g/cm^3, with a range of 0.48 g/cm^3 (Figure 23). 11A varies from 1.51 g/cm^3 to 1.70 g/cm^3, with a range of 0.18 g/cm^3 (Figure 24). 20A/B varies from 1.22 g/cm^3 to 1.88 g/cm^3, with a range of 0.66 g/cm^3 (Figures 25 and 26).

The density values can be correlated with cesium-137 counts to see if there is a relationship between higher densities and more cesium-137 activity. This would be likely given cesium's preference to adsorb to clay particles over sand particles.

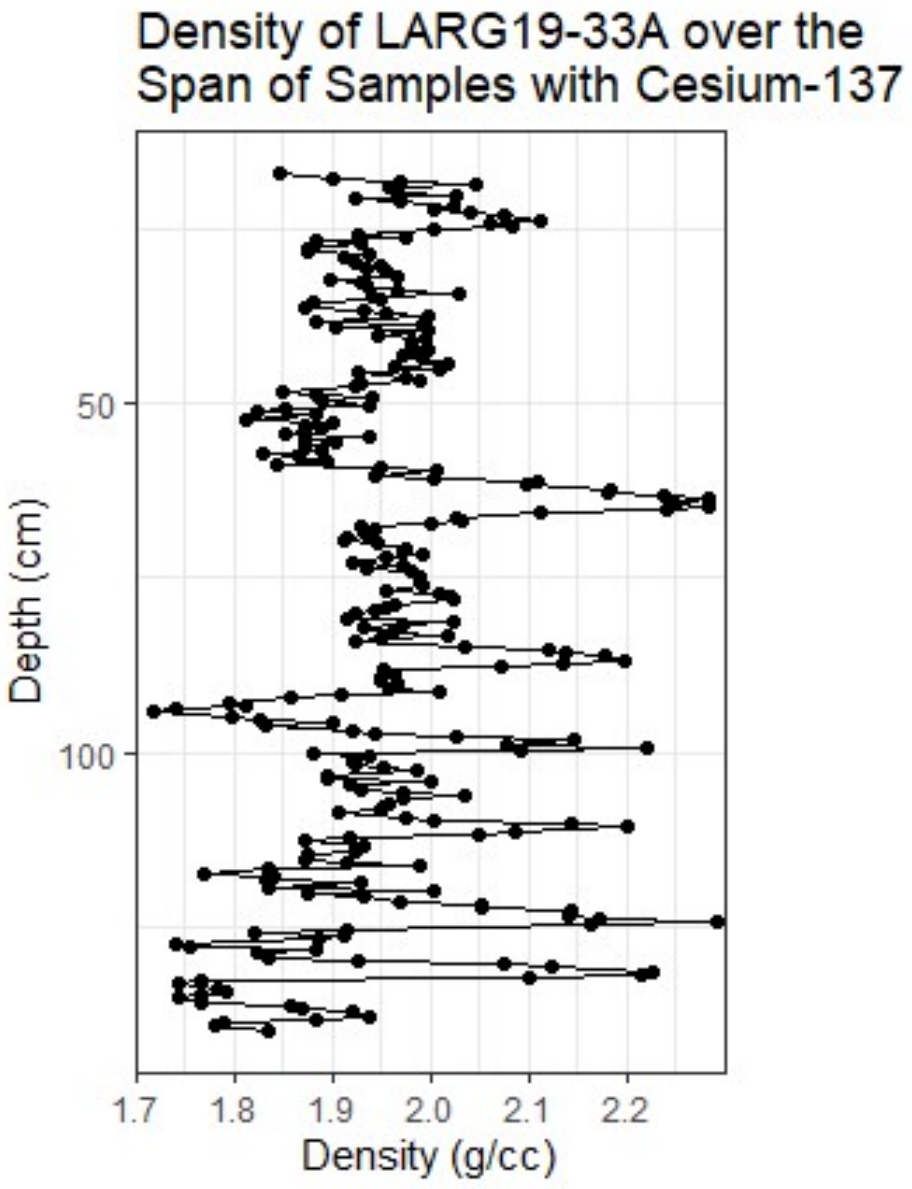

Figure 22: Density plot of LARG19-33A over the span of samples that also had cesium-137 activity.

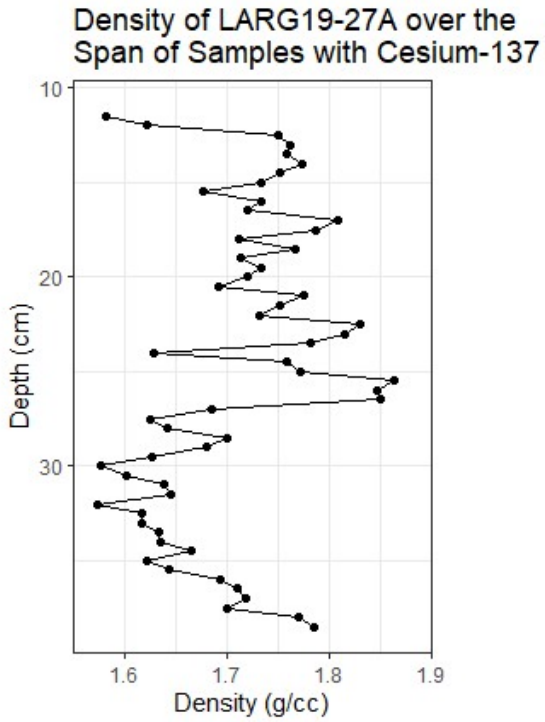

Figure 23: Density plot of LARG19-27A over the span of samples that also had cesium-137 activity.

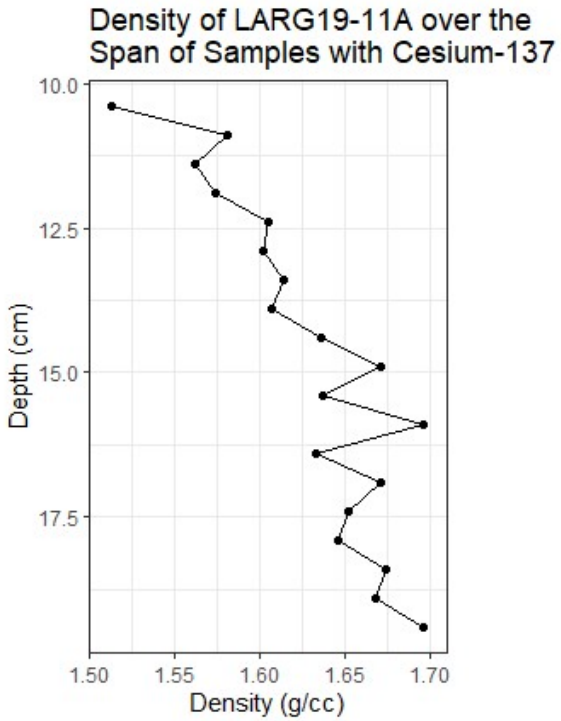

Figure 24: Density plot of LARG19-11A over the span of samples that also had cesium-137 activity.

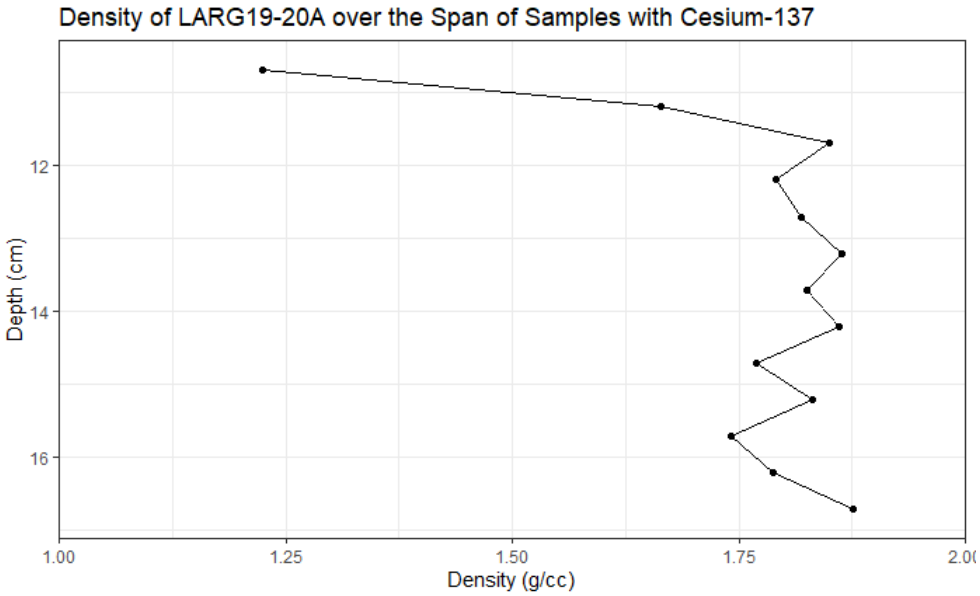

Figure 25: Density plot of LARG19-20A over the span of samples that also had cesium-137 activity.

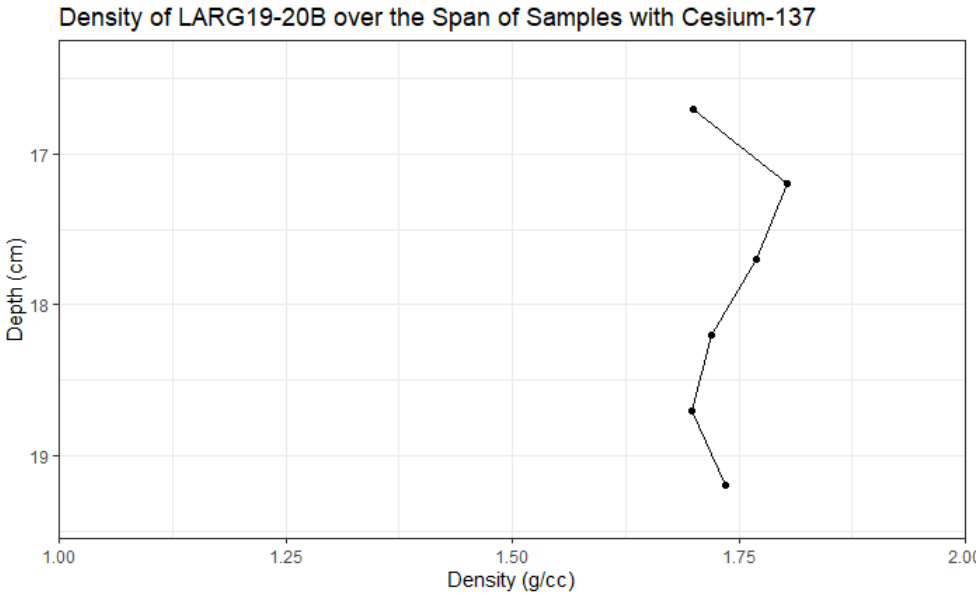

Figure 26: Density plot of LARG19-20B over the span of samples that also had cesium-137 activity.

5.2 Lake Josephine

Two cores were studied, one close to the inlet, the other near the outlet (Figure 27). These particular cores were used because they were the farthest apart across Lake Josephine, while still being in line with the flow of the lake. There were other cores available to use from the north end of the lake, but they did not lie in the channel from the inlet to the outlet river. JOS14-1C (Figure 28) is from the upstream side of Lake Josephine, close to the river input, and JOS10-2A (Figure 29) is near the river output.

Core JOS14-1C had a significant activity peak at a depth of 28 cm, equivalent to a sediment depth of 19 cm. This is equivalent to a sedimentation rate of 3.73 mm/yr using Equation 2. Specific activity increased from a depth of 35 cm to a depth of 28 cm, where it peaked at 5.46 mBq/g. Activity decreased to 26 cm, before showing a lower peak at a depth of 22 cm at 2.71 mBq/g. After this peak, activity gradually decreased to the top of the core (Figure 30).

Another lab, the St. Croix Watershed Research Station, also did cesium-137 analysis of this core. The curves are close, but not identical. However the main reason for variation is that the samples are not from the same depths. The similarities do verify that Macalester College's gamma-ray spectrometer as well as my methods are similar to professional laboratories. The curves differ in magnitude, with my highest value being at 5.46 mBq/g, and the external lab's highest value being at 256.8 mBq/g. This extreme difference is likely due to our detector not being adjusted for relative efficiency, while the other lab's detector was. It is common for labs to not adjust for relative efficiency, given that it is mostly used for relative dating within the core. The major use for accounting for relative efficiency is looking at accumulations of cesium-137 globally, allowing for comparisons spatially. Another major difference between the two lab's results, is where the peak lies. The external lab had a peak activity depth at 25.5 cm core depth, 2.5 cm off from my results. At the moment, I am unsure why there was such a difference, especially when both my peak and the other peak had such strong signals.

Figure 27: Map of Lake Josephine showing the locations of all cores taken, with the pins on the cores used in this study. Core A is JOS14-1C and Core B is JOS10-2A.

Figure 28: Core GNP-JOS14-1C. The top of the core is the left side.

Figure 29: Core GNP-JOS10-2A. The top of the core is the left side.

Core JOS10-2A had a significant activity peak at a depth of 10.5 cm, equivalent to a sediment depth of 1 cm. The sedimentation rate here is estimated to be 0.21 mm/yr. This core showed a gradual increase in cesium-137 specific activity, going from 0 mBq/g at a depth of 15.5 cm, to a peak of 1.45 mBq/g at a core depth of 10.5 cm. There is only one sample taken above this peak, and specific activity only drops to 0.96 mBq/g (Figure 31).

Peak cesium-137 activity in Lake Josephine ranges from 1.45 to 5.46 mBq/g. Sedimentation rates decrease by a factor of 18 from JOS14-1C to JOS10-2A (Table 3).

Density values of JOS14-1C vary between 1.05 and 1.67 g/cm^3 (Figure 32). Density values of JOS10-2A vary between 0.97 and 1.70 g/cm^3 (Figure 33). While density of sediments cannot be below 1 g/cm^3, because that is the density of water, the value of 0.97 is likely due to a measurement of the combination of Zorbitrol and sediment, yielding a density less than 1 g/cm^3. Like in Lago Argentino, the absolute values are of little use. Unlike the Lago Argentino density results, the Lake Josephine density curves look similar, with an increase down the core, with a higher density peak near the middle of the section before it decreases again.

Another core taken, GNP-JOS14-1D-1P, was collected for the purpose of lead-210 dating. Lead-210 dates back about 100 years, giving a slightly longer timescale than cesium-137. Analysis of lead-210 data on this core yields an average sedimentation rate of 3.70 mm/yr. This is slightly lower than the average sedimentation rate of JOS14-1C using cesium-137 dating, which comes out to 3.73 mm/yr.

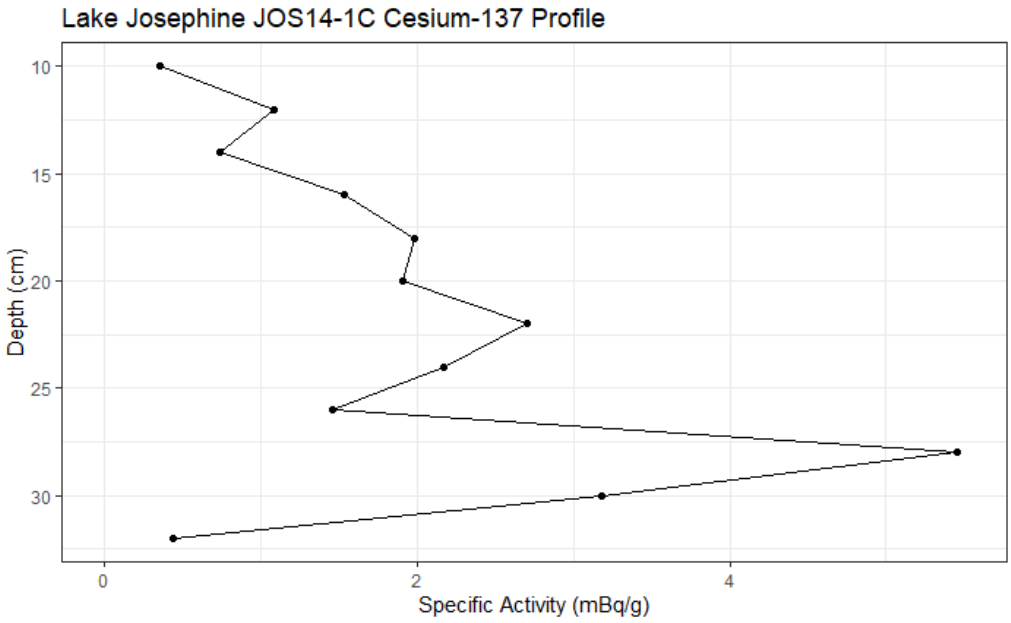

Figure 30: Cesium-137 distribution within core GNP-JOS14-1C-1P

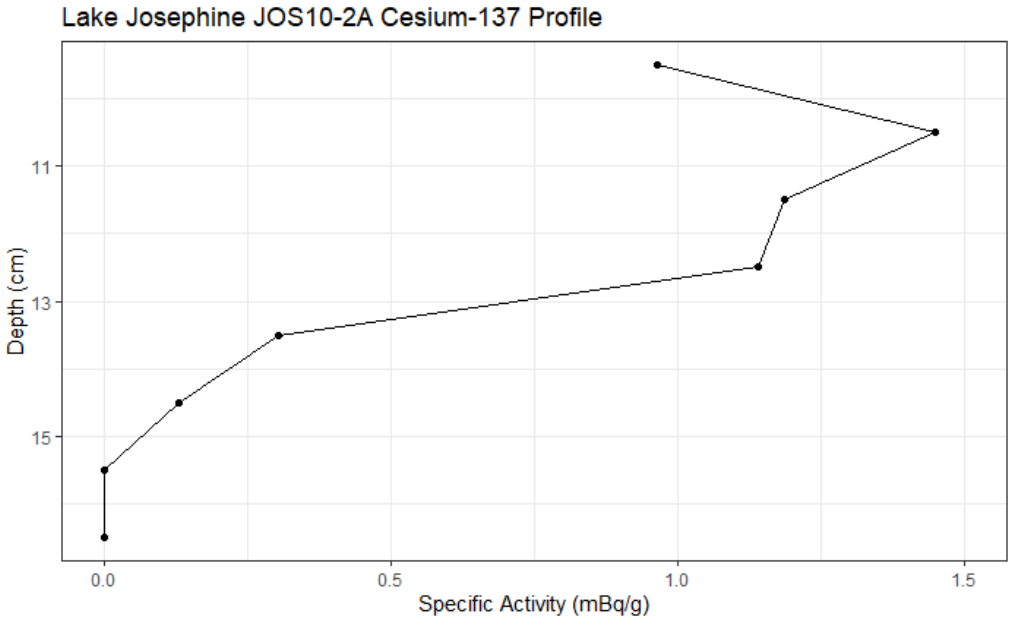

Figure 31: Cesium-137 distribution within core GNP-JOS10-2A-1P

Core	Depth of Activity Peak (cm)	Sedimentation Rate (mm/yr)	Peak Activity (mBq/g)
JOS14-1C	19	3.73	5.46
JOS10-2A	1	0.21	1.45

Table 3: Table summarizing results of Lake Josephine cores.

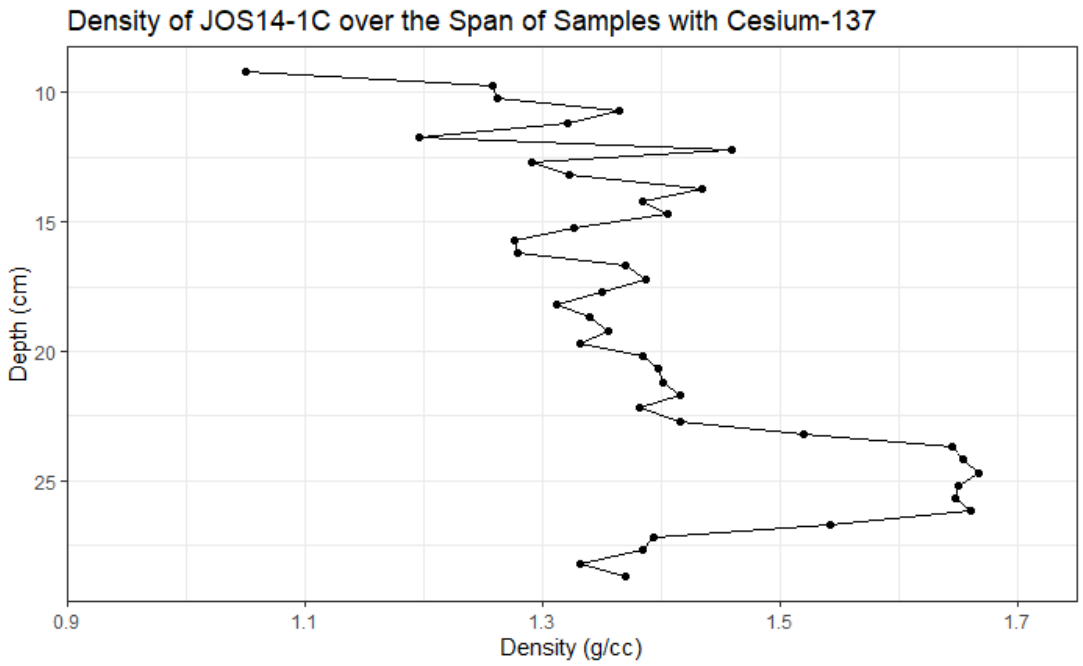

Figure 32: Density plot of JOS14-1C over the span of samples that also had cesium-137 activity.

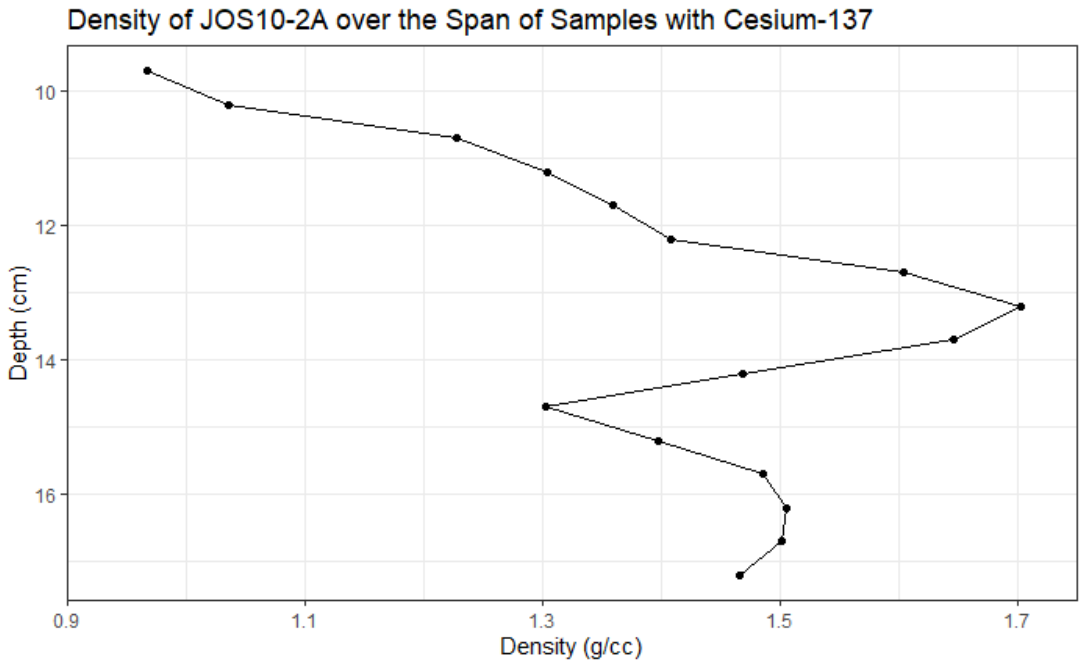

Figure 33: Density plot of JOS10-2A over the span of samples that also had cesium-137 activity.

6 Discussion

6.1 Lago Argentino

As expected, sedimentation rates are higher for locations closer to the sediment influx (Carrivick and Tweed, 2013). The sedimentation rates decrease by a factor of 36 from 33A to 11A, going from 19.4 millimeters per year to 0.54 millimeters per year. This is because there is more sediment present that has been eroded from underneath the glacier, as well as sediment that has fallen on to the glacier. Ice-proximal core sediment (33A) is much coarser than sediment in downvalley cores. This is likely because the combination of water discharge from melting ice and subglacial water flux, and wind creating turbulent currents in near-glacier waters, mean fine sediment can be transported further from the glacier, while coarse material with higher settling velocities fall out of suspension. The finer particles do settle out farther away where there is less energy. Both the side bay (20A/B) and the main basin (11A) have much finer particles, which is evidence of less energy. Here, since energy mainly comes from wind, which causes mixing in the lake layers, there is very little force left from lake inputs, as the location of 11A is over 65 kilometers away from the glacier fronts, and 27 kilometers from the nearest major river input. This is where only the finest of particles settle out. As mentioned in the results, density values in a vacuum are difficult to interpret and not very useful. Here, the overall range in density can be used to get a sense of energy. The range in density decreases as distance from the glacial front increases. This pattern appears again due to there being more energy closer to the glaciers, where more variety in particle sizes can settle out. Farther out into the main basin, where there is very little variability in density, the cores are mostly clay.

Looking at the cores directly, sediments appear to be darker nearer to the glaciers, and lighter farther out, this corresponds with the observation of mafic minerals being segregated into different bands in varves (Van Wyk de Vries et al., 2022). Grain sizes are coarser closer to the glaciers and finer farther away. This

is logical because the near-glacier environment has much more energy with high water input levels than the middle of the basin, where very fine sediments can finally settle out of the lake. By counting varves using countMYvarves, it was revealed that main basin cores had thousands of laminae, while those in the arms had hundreds (Van Wyk de Vries et al., 2021). In the main basin, sediments were typically only microns across, and those in the arms were generally coarser, and contained non-laminated sand layers.

Given a general theoretical cesium-137 profile, the deviations from the theoretical curve can be compared to experimental core activity profiles to speak on events that happened in the lake at certain points in time (Figure 5). The core activity profile having shallower slopes compared to the theoretical curve points to dilution of cesium-137, likely due to higher than normal sedimentation rates. If the core profile is more compact (steeper slopes), it is likely there was less sedimentation over that time interval.

Core 33A has a period of dilution, meaning the actual cesium-137 profile has lower proportional activity than the theoretical activity profile, from approximately 108 cm to 118 cm, where it is much lower than what otherwise would be a taper down from the peak activity. Lithologically, this corresponds with a section that is classified as potentially sandy silt. This is coarser than the surrounding sediments both above and below. Coarser sediment signifies higher energy in the lake, which could be related to an outburst flood that would carry more coarse sediments and would be deposited over a shorter time scale, inflating the average sedimentation rate and diluting the cesium-137 activity. However, coarser sediment also results in less cesium-137 adhesion, which would also artificially dilute cesium-137 activity. This combination of evidence makes it difficult to say if the sediment package from 108 cm to 118 cm in 33A was deposited during an approximate five-year span of higher sedimentation rate, or there happened to be coarser sediment that kept cesium-137 activity down, though the coarse sediment is well explained by the same reason as the decrease in cesium-137 activity. Core 27A and

core 20A/B appear to match this pattern well, and along with consistent grain sizes, leave little room for investigating sedimentation rate variability. Because core 11A had such low resolution due to extremely low sedimentation rates, little can be said about its variability over time. Core 20A/B, due to its location being not along the transect down the lake, is difficult to use for determining overall lake behavior, in addition to containing much more volcanic material than any other core, with tephra and fresh volcanic glass present.

These variations in the profile can also be correlated to past climate data. Warmer time periods would lead to more water coming out of the glacier, diluting the profile. Using the IPCC WGI Interactive Atlas's CRU TS database, the correlation between cesium-137 profile distortion and climate can be investigated. Looking at the dilution core 33A between 108 cm and 118 cm, this period of dilution began about four years after the peak, or 1967. The IPCC CRU TS data shows that the Southern South America region is warmer than average from 1966 to 1970, pointing to the idea that this period of apparent dilution of the cesium-137 profile was caused by warmer weather leading to more melting (Figure 34). Because Lago Argentino is so big, and sedimentation rates decrease so much across it, this climate variation is difficult to see in either of the down-lake cores. Higher resolution of cesium-137 activity would likely yield more climate correlations.

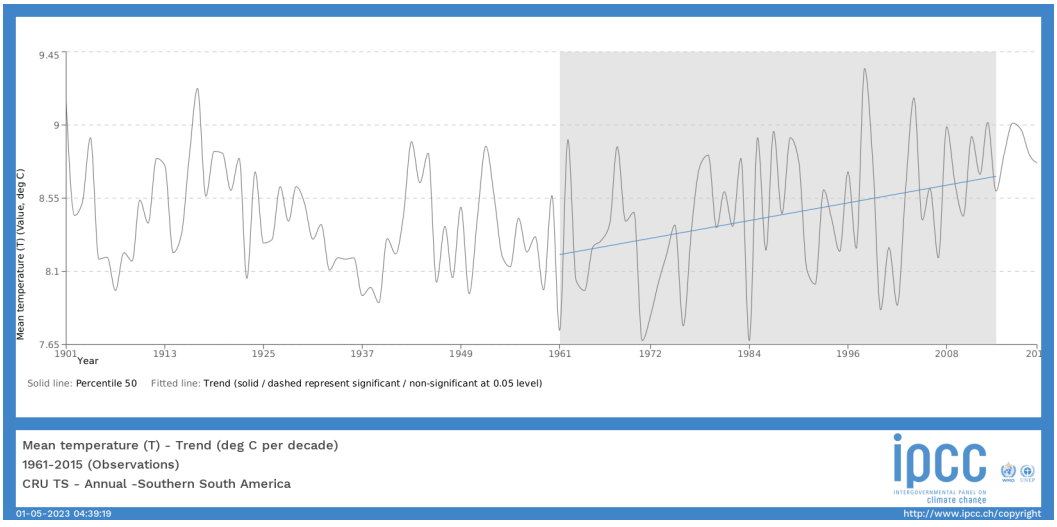

Figure 34: IPCC climate data of Southern South America, showing more years warmer than average (blue line) between 1966 and 1970 (Iturbide et al., 2021).

Because sedimentation represents the amount of sediment being eroded by the glaciers into the lake, the average annual volume of sediment eroded by the glaciers can be calculated by integrating the sedimentation rates over the area of the lake. The pattern of decrease looks to be exponential decay along the transect, though it is difficult to know for sure given only three data points in the transect. Additionally, 33A comes from the lower arm of the lake, and there are no data points from the northern arm analyzed here. This assessment of sedimentation rates being exponential decay does agree with Van Wyk de Vries et al. (2022), which is comparable to ice-contact marine settings (Boldt, 2014).

There have been other studies looking at cesium-137 in lake cores done in South America, and their data can be compared to mine to see how closely they agree. One study was done in Lake Nahuel Huapi (Guevara et al., 2002), and they also concluded that Southern Hemisphere depositional patterns did not match those of the Northern Hemisphere. They also dated the most intense fallout peaks to the period from 1964-1966, which differs from the global average peak date range used by two years (1962-1964). If I were to have used this date range for my data, it would increase the sedimentation rates slightly, by 3.7 percent (Table 4). It is difficult to compare amounts of cesium-137 between the two locations, because of detector efficiencies and radioactive decay. Lake Nahuel Huapi is approximately 1000 kilometers north of Lago Argentino, so the cesium-137 values would be expected to be higher. This expectation is reinforced by atmospheric circulation patterns, since Lake Nahuel Huapi is closer to the meeting point of the Hadley and Ferrel cells than Lago Argentino.

6.2 Lake Josephine

Lake Josephine also saw results as expected. Sedimentation rates decreased by a factor of 18, with 3.73 mm/yr on the upvalley end, and 0.21 mm/yr on the downvalley end. While Lake Josephine is not ice contact, the rivers between lakes transport the sediment eroded by the glacier downvalley. The lake still

exhibits the ability to concentrate sediment deposition at the input end. The pattern of sedimentation rate can only be assumed to be exponential decay like other proglacial lakes, because there were only two data points, so the line of best fit could take any form and still pass through both points. The density-based estimates of grain size are comparable between JOS14-1C and JOS10-2A, both of them range from about 1.05 g/cm^3 to 1.7 g/cm^3. Comparing these to the initial core descriptions yield little additional insight. JOS14-1C has a clay layer at the same depth as the peak in density (24-26 cm of depth), and the rest was defined as a silt. Because JOS10-2A had such a shallow cesium-137 peak, there is not enough resolution in the ICD to pick out any variation along the section of interest, it is just defined as a clay. Visually, the two cores are different, JOS14-1C is dark brown, whereas JOS10-2A is gray, though this likely means nothing of note. Because of the significantly smaller scale, both in terms of lake size and drainage basin size, of Lake Josephine than Lago Argentino, lake behavior is different. Lake Josephine does not need to rely on wind to mix lake layers and give energy to the main basin of the lake, as the river inputs and outputs are comparatively so close together.

Lake Josephine cores can also be compared to the cesium-137 profiles found here to the ones put forth by Cambray et al. (1989), this time using to the Northern Hemisphere curve instead of the Southern Hemisphere curve. It is likely that the upper centimeters of Lake Josephine cores have also been more turbated than Lago Argentino cores because there is vegetation at the bottom of Lake

Core	Sedimentation Rate Based on 1963 (mm/yr)	Sedimentation Rate Based on 1965 (mm/yr)
33A	19.4	20.1
27A	3.39	3.52
11A	0.54	0.56
20A/B	0.80	0.83

Table 4: Table comparing sedimentation rates from global average date to date determined by Guevara et al. (2002) to be the peak date for the Southern Hemisphere.

Josephine, while there is none in Lago Argentino at the depths cores were taken from. The upper portions of Lake Josephine cores may also have been affected by different groups taking the samples than the group that took the Lago Argentino cores. Core JOS14-1C matches the profile fairly well, showing a strong peak (The two peaks in Figure 5 are likely too close together to see with any distinction), a decrease, then another spike, likely representing the Chernobyl Disaster, before it semi-linearly decreases to present. Core JOS10-2A had the lowest sedimentation rate of all cores analyzed, with resolution far too low to relate to any events shown in Figure 5. However, it does have a very wide peak, wider than peaks seen in cores with three times greater sedimentation rates. The cause for this is unknown, but it does not represent continued cesium-137 fallout. A potential cause could be the blending of the 1963 peak with the Chernobyl peak.

While glaciers dominate the erosional landscape in Glacier National Park, the rivers between the paternoster lakes might potentially also erode the landscape. This would interfere with the assumption that all sediment occurring in downvalley lakes comes from glacial erosion, thus making the lake sedimentation rate to glacial erosion rate convoluted. Glacial erosion rates, though, are typically an order of magnitude higher than fluvial erosion rate. MacGregor et al. (2011) found that certain conditions are necessary to transport dolomite, which is only present up at the top of the valley where Grinnell Glacier sits, to Swiftcurrent Lake, which is the lake immediately downvalley of Lake Josephine. This likely translates to Lake Josephine to some extent, that not much of the material actually eroded by Grinnell Glacier ends up in the lake, instead being deposited in the lakes upvalley of Lake Josephine. This makes it difficult to estimate fully the amount of erosion done by Grinnell Glacier per year. Additionally, Grinnell Glacier has shrunk significantly over the past 100 years, and there is repeat photography starting in 1910 showing that. Back when the first picture was taken, there was no Upper Grinnell Lake, the glacier entirely covered the place where the lake now stands.

Previous age dating of JOS14-1D was conducted to constrain historical sed-

imentation rates (MacGregor, unpublished data). The sedimentation rate estimated by lead-210 dating was 0.03 mm/yr less than that determined by cesium-137 dating (3.70 mm/yr since. This difference is too slight to draw any meaningful conclusions But it still points to consistent erosion and melting rates from about 1900-1960 as 1960 to the present. This result was surprising, as higher rates of melting of the Grinnell Glacier more recently in time would be expected to be reflected in the sedimentation rates. Higher melt rates would be expected to lead to higher sedimentation rates, as there would be more water carried down-basin, leading to more sediment being carried into the non-ice-contact lakes. On the other hand, melting glaciers lead to less erosion done by the glacier, which results in less sediment in the lake system.

Comparing the sedimentation rates in JOS14-1C to the IPCC CRU TS data is difficult, as it has low sedimentation rates with relatively low resolution of specific activity, but the shorter than expected (based on average sedimentation rates) gap in between the 1963 and mid-1980's Chernobyl peak does correspond with lower than average temperatures in the Western North America region (Figure 35).

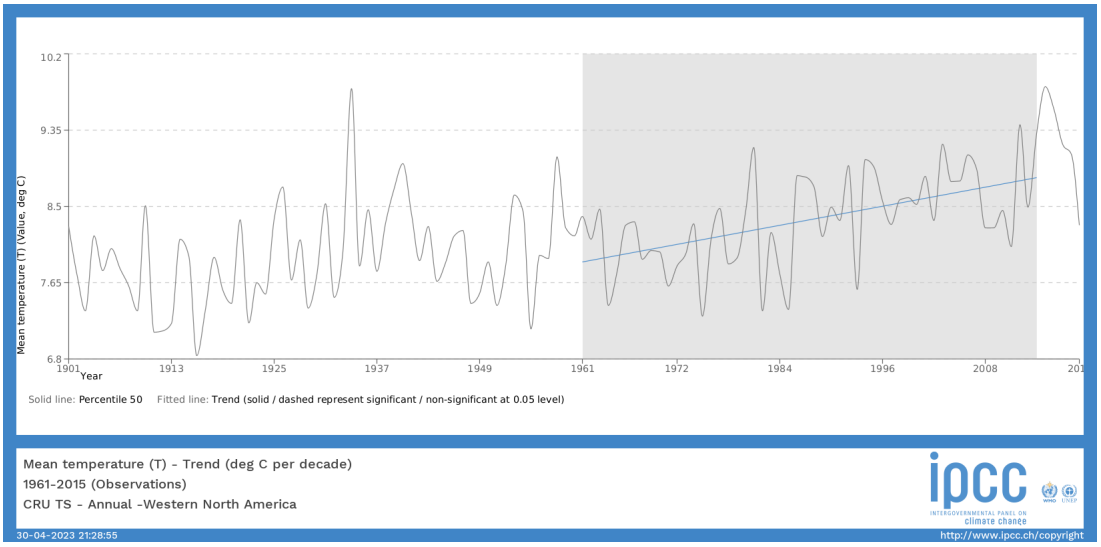

Figure 35: IPCC climate data of Western North America, showing more years colder than average (blue line) between 1963 and the mid-1980's (Iturbide et al., 2021).

6.3 Comparison

Lago Argentino and Lake Josephine differ in local geography, size, and glacier proximity, but both lakes can be compared in terms of sediment dynamics to see if there are any similarities between the two. Both lakes see over an order of magnitude difference in sedimentation rates from the upvalley to the downvalley ends of the lakes. Sedimentation rates in Lago Argentino closer to the glacier front are 36 times higher than those in the main basin, and Lake Josephine's are 18 times higher near the inlet than the outlet. Despite Lago Argentino being over 2,700 times larger than Lake Josephine in terms of surface area, the decrease in sedimentation rates is only twice as much as Lake Josephine. This is surprising, because of the magnitudes of difference in size, that particles still fall out of suspension at the same rate. The total sediment output is much larger in Lago Argentino due to more, and much larger, glaciers providing the sediment influx. Because Lago Argentino is so much bigger than Lake Josephine, there is more area for sediment to be deposited.

Sedimentation rates within proglacial lakes have been measured throughout the world, and these can be compared to others to determine global trends. Lake Qiangyong Co in southern Tibet is another small (0.08 km^2), paternoster (second in the chain), proglacial lake that underwent lead-210 and cesium-137 dating to determine sedimentation rates (Zhang et al., 2021). This study found that the sedimentation rates on the upvalley side of the lake were 2.1 mm/yr, compared to the center of the lake where they were approximately half of that. Zhang et al. (2021) did not publish the locations of their cores, but based on the description of cores being taken from near the inlet and in the middle of the basin, the distance between the cores can be estimated to be between 150 and 200 m apart. While this decrease is significantly less than that of larger Lake Josephine, the basin geometry may also play a role in comparing lake area to sedimentation rate decrease. Lake Qiangyong Co is 350 m across, while Lake Josephine is nearly 1,200 m from inlet to outlet. From core to core, the Lake Josephine cores are 830 m apart.

The Northern Hemisphere cores have a proportionally higher second pulse of cesium-137 concentrations. This second pulse is the representation of the Chernobyl disaster in the mid-1980s. Because this event was confined to the Northern Hemisphere, there was very little transfer of radionuclide particles to the Southern Hemisphere. The average specific activity of cesium-137 in Lago Argentino was 0.47 mBq/g, and it was 3.46 mBq/g in Lake Josephine. The actual numbers don't match the numbers from Agudo et al. (1998) (Figure 3). This difference is due to nuclear decay since 1998 and comparative detector efficiency. Agudo et al. (1998) estimated the cesium-137 activity to be around 40 mBq/cm^2 near Lago Argentino, and around 280 mBq/cm^2 near Lake Josephine. Both my data and that of Agudo et al. (1998) have specific activity being about seven times higher in Lake Josephine than in Lago Argentino.

7 Conclusions

Overall, I found that sedimentation rates decreased from 19.4 mm/yr to 0.54 mm/yr along a 47-kilometer-long transect in Lago Argentino, from 3.73 mm/yr to 0.21 mm/yr along a 830-meter-long transect in Lake Josephine. These decreases are in the same order of magnitude, a factor of 36 versus a factor of 18. Despite Lago Argentino being 2,700 times larger than Lake Josephine in terms of surface area, Lago Argentino being ice-contact and Lake Josephine being paternoster, and the climates and landscapes of each glacial lake being vastly different, they have similar rates of sedimentation. As a corollary, glaciers erode sediment at similar rates despite these massive differences.

The Southern Patagonian Icefield is undergoing some of the highest rates of uplift in the world, with maximum uplift rates exceeding 4 centimeters per year (Richter et al., 2016). This is incredibly fast geologically speaking, and is caused by the continued uplift of the Andes, but also isostatic rebound from melting glaciers. Because of this, it is very difficult to measure glacial erosion with standard

techniques like GPS. Calculating the sedimentation rate then serves as a proxy for how much material the glacier is eroding from the bedrock

This research is important because sedimentation rates can track erosion, and in the case of proglacial lakes, it is the erosion of glaciers, which is often used as a proxy for climate change. In areas with significant tectonic or isostatic uplift, glacial erosion can be difficult to measure using standard GPS methods, so sedimentation rate can be used to estimate how much of the glacier is being eroded from the amount of water melted off. Varve counting has been used to track sedimentation rates, although laminations in glacial lake sediments are not always annual varves, so cesium-137 analysis can be used to confirm varve counts.

Additionally, both the Southern Patagonian Icefield and Grinnell Glacier are shrinking. Glaciar Upsala in the SPI has retreated at least 4.3 km since 1995 (Moragues et al., 2017). Grinnell Glacier shrank from 2.33 km^2 in 1850, to 0.88 km^2 in 1993 (Key et al., 2002).

Cesium-137 is confirmed to be an effective tool for dating sediments with relatively high rates of accumulation, especially if research is only interested in the past 60 years, as it is more straightforward and cheaper than other techniques. The process for dating sediments does not require complicated chemistry with hazardous chemicals like zircon dating, nor does it require understanding of historical trends like carbon-14 dating. It only requires the detection of maximum specific activity in the depth of the core. After startup costs for the spectroscopy device, the only continuing costs are for liquid nitrogen to keep the detector cooled.

Further understanding of how cesium-137 behaves in glacial lake sediments as far as distribution could have implications for remediation and clean up of lakes contaminated with heavy metals like cesium-137 that preferentially adsorb to fine particles.

8 Acknowledgments

I would like to thank many people and groups for getting me here and supporting me along the way: My friends and family, for supporting me over my past four years at Macalester college, especially over the years impacted by COVID, The geology department as a whole, whose amazing culture made me feel accepted since the moment I declared my major, My advisor, Dr. Kelly MacGregor, for supporting me along my geology academic career and giving me the opportunity to do amazing research, The Keck Consortium, for allowing me to go to Glacier National Park to experience geological fieldwork, Past Keck researchers, for collecting Lake Josephine cores, Support provided by the Continental Scientific Drilling Facility, University of Minnesota, for collecting Lago Argentino cores and providing equipment and lab support for Lake Josephine cores, The Blackfeet Nation, for on whose ancestral lands we conducted our research in current-day Glacier National Park, The National Science Foundation, for funding this research under Grant No. EAR-1714614, coordinated by Lead PI Maria Beatrice Magnani. This material is based upon work supported by the Keck Geology Consortium and the National Science Foundation under Grant No. 2050697

9 Works Cited

[1] E. Garcia Agudo. Global distribution of 137cs inputs for soil erosion and sedimentation studies. In *IAEA*, pages 117–121, Vienna, Sep 18, 1998 Jul 1, 1998. International Atomic Energy Agency.

[2] Glacier Natural History Association. Glaciers and glaciation in glacier national park, July 11, 2008.

[3] Katherine Boldt. *Fjord sedimentation during the rapid retreat of tidewater glaciers: observations and modeling.* PhD thesis, Jan 1, 2014.

[4] R. S. Cambray, K. Playford, G. N. J. Lewis, and R. C. Carpenter. Radioactive

fallout in air and rain: results to the end of 1987. *Harwell, Eng., Atomic Energy Establishment, AERE-R 13226, June, 1989*, page 20, Jun 1, 1989.

[5] Jonathan L. Carrivick and Fiona S. Tweed. Proglacial lakes: character, behaviour and geological importance. *Quaternary science reviews*, 78:34–52, Oct 15, 2013.

[6] Isabelle Coutand, Marc Diraison, Peter R. Cobbold, Denis Gapais, Eduardo A. Rossello, and Muriel Miller. Structure and kinematics of a foothills transect, lago viedma, southern andes (49°30s). *Journal of South American earth sciences*, 12(1):1–15, 1999.

[7] Maximillian Van Wyk de Vries, Emi Ito, Mark Shapley, and Guido Brignone. Semi-automated counting of complex varves through image autocorrelation. *Quaternary research*, 104:89–100, Nov 1, 2021.

[8] Maximillian Van Wyk de Vries, Emi Ito, Mark Shapley, Guido Brignone, Matias Romero, Andrew D. Wickert, Louis H. Miller, and Kelly R. MacGregor. Physical limnology and sediment dynamics of lago argentino, the world's largest ice-contact lake. *Journal of geophysical research. Earth surface*, 127(3):n/a, Mar 2022.

[9] Emily Diener. *Inorganic Carbon in an Alpine Lake as a Proxy for Glacier Dynamics during the Late Holocene, Glacier National Park, Montana.* PhD thesis, April 29, 2015.

[10] CSD Facility. Coring and drilling systems, 2023.

[11] Nicolas Fourches, Magdalena Zielinska, and Gabriel Charles. High purity germanium: From gamma-ray detection to dark matter subterranean detectors, Mar 29, 2019.

[12] Geotek. Mscl sensors, 2023.

[13] S. Ribeiro Guevara and M. Arribere. (super 137) cs dating of lake cores from the nahuel huapi national park, patagonia, argentina; historical records and profile measurements. *Journal of Radioanalytical and Nuclear Chemistry*, 252(1):37–45, 2002. Source type: Scholarly Journals; Object type: Article; Copyright: GeoRef, Copyright 2020, American Geosciences Institute.; CSAUnique: 2002-080713; AccNum: 2002-080713; ISSN: 0236-5731; CODEN: JRNCDM; Peer Reviewed: true.

[14] Shoji Hashimoto, Masabumi Komatsu, and Satoru Miura. Booklet to provide basic information regarding health effects of radiation, March 31, 2013.

[15] M. Iturbide, J. Fernández, J.M. Gutiérrez, J. Bedia, E. Cimadevilla, J. Díez-Sierra, R. Manzanas, A. Casanueva, J. Baño-Medina, J. Milovac, S. Herrera, A.S. Cofiño, D. San Martín, M. García-Díez, M. Hauser, D. Huard, and Ö. Yelekci. Repository supporting the implementation of fair principles in the ipcc-wg1 atlas., 2021.

[16] Carl Key, Daniel Fagre, and Richard Menicke. Glacier retreat in glacier national park, montana. Technical report, USGS, Jan 2002.

[17] Daryl Kimball. The nuclear testing tally, August 2022.

[18] Grahame Larson and Randall Schaetzl. Origin and evolution of the great lakes. *Journal of Great Lakes research*, 27(4):518–546, 2001.

[19] Maria P. Iglesia Llanos, Roberto Lanza, Alberto C. Riccardi, Silvana Geuna, Marinella A. Laurenzi, and Raffaella Ruffini. Palaeomagnetic study of the el quemado complex and marifil formation, patagonian jurassic igneous province, argentina. *Geophysical Journal International*, 154(3):599–617, 2003.

[20] K. R. MacGregor, R. S. Anderson, S. P. Anderson, and E. D. Waddington. Numerical simulations of glacial-valley longitudinal profile evolution. *Geology (Boulder)*, 28(11):1031–1034, Nov 1, 2000.

[21] Peter Van Metre, Jennifer Wilson, Christopher Fuller, Edward Callender, and Barbara Mahler. Collection, analysis, and age-dating of sediment cores from 56 u.s. lakes and reservoirs sampled by the u.s. geological survey, 1992-2001, 2004.

[22] Silvana Moragues, M. Gabriela Lenzano, Andres Lo Vecchio, Daniel Falaschi, and Luis Lenzano. Surface velocities of upsala glacier, southern patagonian andes, estimated using cross-correlation satellite imagery: 2013-2014 period, Jan 1, 2018.

[23] Damián Moyano-Paz, Camila Tettamanti, Augusto Varela, Abril Cereceda, and Daniel Poiré. Depositional processes and stratigraphic evolution of the campanian deltaic system of la anita formation, austral-magallanes basin, patagonia, argentina. *Latin American Journal of Sedimentology and Basin Analysis*, 25:69–92, Dec 8, 2018.

[24] A. J. M. Plompen, O. Cabellos, C. De Saint Jean, and M. Fleming. Jeff-3.1, 2006.

[25] A. Revil, D. Grauls, and O. Brévart. Mechanical compaction of sand/clay mixtures. *Journal of Geophysical Research - Solid Earth*, 107(B11):ECV 11–15, Nov 2002.

[26] A. Richter, E. Ivins, H. Lange, L. Mendoza, L. Schröder, J. L. Hormaechea, G. Casassa, E. Marderwald, M. Fritsche, R. Perdomo, M. Horwath, and R. Dietrich. Crustal deformation across the southern patagonian icefield observed by gnss. *Earth and planetary science letters*, 452:206–215, Oct 15, 2016.

[27] Catherine A. Riihimaki, Kelly R. MacGregor, Robert S. Anderson, Suzanne P. Anderson, and Michael G. Loso. Sediment evacuation and glacial erosion rates at a small alpine glacier. *Journal of Geophysical Research*, 110(F3):F03003–n/a, Sep 2005.

[28] Nathan S. Schachtman, Kelly R. MacGregor, Amy Myrbo, Nora Rose Hencir, Catherine A. Riihimaki, Jeffrey T. Thole, and Louisa I. Bradtmiller. Lake core record of grinnell glacier dynamics during the latest pleistocene deglaciation and the younger dryas, glacier national park, montana, usa. *Quaternary research*, 84(1):1–11, Jul 2015.

[29] National Park Service. Geology of glacier national park, Sep 21, 2020.

[30] Jorge A. Strelin, Michael R. Kaplan, Marcus J. Vandergoes, George H. Denton, and Joerg M. Schaefer. Holocene glacier history of the lago argentino basin, southern patagonian icefield. *Quaternary Science Reviews*, 101:124–145, 2014. Source type: Scholarly Journals; Object type: Article; Copyright: GeoRef, Copyright 2020, American Geosciences Institute. Reference includes data from CAPCAS, Elsevier Scientific Publishers, Amsterdam, Netherlands; CSAUnique: 2015-056828; AccNum: 2015-056828; ISSN: 0277-3791; DOI: 10.1016/j.quascirev.2014.06.026; Peer Reviewed: true.

[31] Darrel A. Swift, Simon Cook, Tobias Heckmann, Jeffrey Moore, Isabelle Gärtner-Roer, and Oliver Korup. *Chapter 6 - Ice and Snow as Land-Forming Agents*, pages 167–199. Snow and Ice-Related Hazards, Risks, and Disasters. Elsevier Inc, 2015.

[32] Run Zhang, Jin Zhangdong, Fei Zhang, Zhang Xiaolong, Li Liangbo, Xu Yang, and Xu Baiqing. Sedimentation rate variations of the proglacial lake (qiangyong co) and its implications for glacial fluctuations over the past century, southern tibet, china. *Hupo Kexue (Journal of Lake Sciences)*, 33(5):1584–1594, Sep 6, 2021.